Minimizing Thickness Variation in the Vacuum Infusion (VI) Process with 1D and 2D Resin Flows

by

Talha Akyol

A Thesis Submitted to the

Graduate School of Engineering

in Partial Fulfillment of the Requirements for

the Degree of

Master of Science

in

Mechanical Engineering

Koc University

July 2012

Koc University

Graduate School of Sciences and Engineering

This is to certify that I have examined this copy of a master's thesis by

Talha Akyol

and have found that it is complete and satisfactory in all respects,

and that any and all revisions required by the final

examining committee have been made.

Committee Members:

_____

Murat Sözer, Ph. D. (Advisor)

_____

Erdem Alaca, Ph. D.

_____

Halil Bayraktar, Ph. D.

Date: _____

ABSTRACT

In the Vacuum Infusion (VI) process, the thickness of a composite part changes as the resin pressure, and thus the compaction pressure changes as a function of spatial coordinates and time since the upper mold part is a non-rigid vacuum bag. To manufacture composite parts with small tolerances in thickness, one must know the coupled effect between the resin flow and fabric compaction.

For 1D experiments, pressure and thickness were monitored along resin flow using pressure transducers and non-contact laser displacement sensors. For 2D experiments, thickness was monitored at multiple points using a scanning non-contact laser displacement sensor. To decrease the thickness variation in the controlled version of the repeated VI experiments, some control actions were taken by adjusting the injection boundary conditions such as opening/closing injection gates and ventilation ports and changing their pressures in the post-mold filling stage. The control actions were taken based on an available decompaction database for the fabric type used in this study. For 1D experiments, of a conventional VI process, maximum percentage thickness variation was measured as 5.44%. By applying control actions in post filling stage, the maximum percentage variation was decreased to 0.34%. For 2D experiments, uncontrolled experiments yielded 34.3% maximum thickness variation. Controlled experiments had 7.3% maximum thickness variation. This study concludes that by applying control actions at post filling stage, composite parts with considerably reduced thickness variation can be manufactured. Control Actions must be taken based on compaction and permeability databases constructed in material characterization experiments.

ÖZET

Vakum İnfüzyon (Vİ) yönteminde, kompozit parçanın kalınlığı reçine basıncı ile değişir, böylece üst kalıp parçası katı olmayan bir vakum torbası olduğu için sıkıştırma basıncı uzaysal kordinatların ve zamanın fonksiyonu olarak değişir. Düşük kalınlık toleranslı kompozit parça üretebilmek için reçine akışı ve elyaf sıkıştırlıması arasındaki bileşik etki bilinmelidir.

Bir boyutlu deneyler için, reçine akışı yönünde basınç transdüsörleri ve temassız lazer deplasman sensörleri kullanılarak basınç ve kalınlık takip edildi. İki boyutlu deneyler için, kalınlık, haraket eden temassız lazer deplasman sensörü kullanılarak pek çok notkada kontrol edildi. Kalınlık varyasyonunu düşürmek için kapıları açmak/kapamak, dolum sonrası aşamada kapı basınçlarını değiştirmek, ve fazla reçineyi dışarı akıtmak gibi enjeksiyon parametreleriyle oynayarak kontrol aksiyonları alındı. Kontrol aksiyonları seçimi için önceki çalışmalardan elde edilmiş sıkıştırma/rahatlatma veritabanı kullanıldı. Bir boyutlu deneylerde, normal bir vakum infüzyon işlemi için maksimum kalınlık varyasyonu deneysel olarak %5.44 olarak bulundu. Benzer bir parçaya dolum sonrasında kontrol aksiyonları uygulandığında kalınlık varyasyonunun %0.34'e düştüğü gözlemlendi. İki boyutlu deneylerde kontrol aksiyonu uygulanmamış bir parça %34.3 maksimum kalınlık varyasyonu gösterdi. Kontrol aksiyonu uygulanan durumlarda en düşük kalınlık varyasyonu %7.3 olarak gözlemlendi.. Bu çalışmanın sonucu, kontrol aksiyonu uygulanarak elde edilen parçaların daha düşük kalınlık varyasyonuna sahip olduğunu göstermektedir. Kontrol aksiyonları, karakterizasyon deneylerinden elde edilmiş sıkıştırma ve geçirgenlik veritabanları kullanılarak seçilmelidir.

ACKNOWLEDGEMENTS

I would like to thank my advisor Murat Sözer for all his help and guidance in my studies for these two years. His positive attitude and encouragement played a very major role in my achievements and in the completion of this graduate study. I would also like to thank Assoc. Prof. Erdem Alaca and Assist. Prof. Halil Bayraktar for their participation in the thesis committee.

During this study, I had the chance to work one of the friendliest environment that can be found. I would like to gratefully thank to my Lab colleagues, Bekir Yenilmez, Mustafa Haboğlu, Barış Çağlar, Mehmet Akif Yalçınkaya, and Ayşen Sarıoğlu for the support and friendship they provided. I would like to extend my thanks to Utku Boz, Engin Çukuroğlu, Berkay Yarpuzlu, Berkay Gümüş for their friendship during my studies.

Finally I would like to thank to my father Erol Akyol, my mother Nimet Akyol and to my brother Baran Akyol for their guidance, supports, patience and help during my whole academic and social life.

TABLE OF CONTENTS

LIST OF TABLES

LIST OF FIGURES

NOMENCLATURE

ϕ	Porosity of the fabric
$\rho_{sup,core}$	Superficial density of the core [kg/m^2]
$\rho_{sup,fabric}$	Superficial density of the fabric [kg/m^2]
$\rho_{glass\ fiber}$	Density of the glass fiber [kg/m^3]
$\rho_{polyester}$	Density of the polyester [kg/m^3]
μ	Viscosity [Pa.s]
$\mu_{polyester}$	Viscosity of the polyester [Pa.s]
a	Fabric numerical constant
b	Fabric numerical constant
h	Thickness of the fabric preform [m]
h_m	Height of the mold cavity [m]
h_{si}	Height of the fabric at each sensor, i
i	Index of sensors
Δh	Change in thickness [mm]
L	Length of the fabric preform [m]
k	Kozeny constant [m^2]
K	Permeability of the preform [m^2]
m	Numbers of core fabric
$m_{100\ \%\ fiber}$	Total mass if the mold cavity could be fully with glass fibers [kg]
m_{core}	Mass of the core [kg]
m_{fabric}	Mass of the fabric [kg]
$m_{preform}$	Mass of the preform [kg]
n	Numbers of stitched-random fabric
P	Resin pressure [Pa]
P_{atm}	Atmospheric pressure [Pa]
P_{comp}	Compaction pressure on fabric [Pa]
P_{inj}	Injection pressure in the RTM mold [Pa]
P_{si}	Pressure of the each sensor, i [Pa]

P_{vacuum}	Vacuum pressure [Pa]
Q	Flow rate of the resin [m^3/s]
u	1-D superficial velocity of the resin in x-direction [m/s]
$\overline{u}$	Volume averaged resin velocity [m/s]
u_f	Velocity of the flow front [m/s]
t	Time [s]
x_i	Initial position of the flow front [m]
x_f	Position of the flow front at a certain time [m]
v_f	Fiber volume fraction
w_m	Width of the mold cavity [m]

CHAPTER 1

INTRODUCTION

1.1 Vacuum Infusion (VI) Process

Vacuum Infusion (VI, a.k.a. Vacuum Assisted Resin Transfer Molding, VARTM), is a type of Liquid Composite Molding (LCM) process, which is used to manufacture large fiber-reinforced thermoset matrix composite parts. The reinforcing preform, which is usually made by stacking fabric layers of continuous (or sometimes short random) glass or carbon fibers, is compacted in between a single-sided rigid mold part and a vacuum bag. A vacuum pump evacuates the air from the sealed mold cavity; and thus the difference between the outer pressure (= atmospheric pressure, P_{atm}) and the inner pressure of the mold cavity (= vacuum pressure, P_{vacuum}) acts as the compaction pressure, $P_{compaction}$ on the vacuum bag and the fabric preform:

$$P_{compaction} = P_{atm} - P_{vacuum}. \quad (1)$$

A distribution medium (a.k.a. flow mesh or core material) is also placed in the mold cavity either between the fabric preform and the vacuum bag, or embedded in between fabric

layers; the former use allows one to dispose the distribution medium after demolding, however in the latter version, the distribution medium becomes a permanent part of the composite part. Vacuuming does not only allows the compaction of the fabric preform, but also drives the liquid thermoset resin from a reservoir into the mold cavity due to the pressure gradient created. During the mold filling, the inner pressure becomes the resin pressure in the resin-filled regions, and it is a function of spatial coordinates and time: $P = P(x,y,z,t)$ (however, z-dependence is usually neglected for thin parts). Thus, as the resin pressure increases with time at a fixed spatial coordinate, the compaction pressure at that location decreases with time:

$$P_{compaction}(x,y,t) \quad = \quad P_{atm} - P(x,y,t). \qquad (2)$$

This is the major cause of the thickness variation in the VI process as previously studied in [1,2]. The thickness will not only vary as a function of time, but it will also vary in spatial coordinates since the resin pressure is maximum at the inlet and minimum at the ventilation ports, and varying in between them spatially. It will be a difficult task to manufacture a composite part with tight dimensional tolerances in thickness if the manufacturing engineer relies only on experience and trial-and-error approach, as usually done on the manufacturing floor. In this study, control actions were taken by opening and closing gates/vents and changing the pressure values at the boundary to influence the compaction of the fabric preform and thus trying to minimize the thickness variation in the composite part. The control actions were based on the compaction/decompaction database [2] of the fabric preform used in this study.

CHAPTER 2

LITERATURE REVIEW

2.1 Introduction

The simplest action to reduce the variation in thickness is the application of bleeding. After the mold filling is completed, the inlet gates are closed while keeping the ventilation port(s) open at the vacuum pressure. At the steady state, the resin pressure in the mold becomes constant and equal to the vacuum pressure, which causes the overall thickness to decrease relative to the pre-bleeding values. In the conventional resin-bleeding application, the bleeder material will absorb the excess resin while the resin is being squeezed out of the compacted fabric preform. As experimentally observed in [3], there will still be 4 to 8 % variation in the thickness after the bleeding, which could not be eliminated unless an extra control action is taken. Yenilmez and Sozer [2,4] showed that the compaction of a fabric preform is time-dependent under a constant load. Even under static loading for 15 minutes, the steady state in the thickness could not be achieved for three types of fabrics used in that study. Thus, the thickness variation cannot be totally eliminated by resin bleeding even if the final compaction pressure is constant everywhere. The reason behind this is that, each region has different loading history, resulting in different final thicknesses.

This is also supported by Simacek et al. [18]. In their first scenario, after mold filling, injection is kept open while vent is closed. Additional resin is allowed to enter the system. The system is kept slightly below atmospheric pressure. Settling time for pressure and thickness is simulated to be 4000 seconds. In their second scenario a bleeding action is observed. The initial pressure that is affecting the settling time is much greater in this second scenario than the previous one. As a result the settling time for pressure and thickness is simulated to be 100 seconds, forty times faster than the previous case. This 4000 seconds settling time in [18] supports time dependence of fabric compaction. As it is not straightforward to control the thickness of especially large parts, various experimental monitoring schemes, characterization models and simulations have been studied in the literature, and they will be summarized below.

2.2 Sensors

Commonly used methods for thickness monitoring include using (i) dial gages, (ii) linear variable differential transducers (LVDT), (iii) laser displacement sensors, (iv) digital speckle photography (DSP), and (v) 3D scanners. Dial gages and LVDTs are very similar in principle; and also their accuracy is comparable (dial gages have 10 □m [1] and LVDTs have 12.5 □m [5] accuracy in some published VI applications). They both measure thickness by mechanical contact, thus they apply a local force at the measurement point and this may change the actual compaction pressure there especially, when the actual compaction pressure is low. To reduce the effect of this force, small plates (feet) are used [1,5,6] at the measurement point to distribute the load applied by the tip of the dial gage/LVDT, keeping

the contact pressure at negligible levels. The downside of using these plates is that the sensor measures an average thickness of the part under the feet, which may lead to miss the lubrication effect during rapid flow progression near that location. As studied in [1,2], the lubrication effect explains the transient decrease in thickness even when the compaction pressure starts decreasing upon resin arrival. Thus, one would mistakenly expect the thickness to increase, (i.e., not to decrease) upon resin arrival if the lubrication effect is not taken into account. Laser displacement sensors measure the thickness at a single location similar to dial gages and LVDTs, however, they do not make mechanical contact; rather they measure the distance with the sensor using a laser beam. Since they do not disturb the preform, true local measurements can be done with higher resolution (typically 1.5 μm) compared to LVDTs and dial gages. On the other hand, laser sensors require diffusive surface on the part being measured, so either opaque tape as in this study or spray paint [7] must be applied at measurement points on the vacuum bag. Kessels et al. [7] mounted a laser sensor on a rail and measured the thickness of a part along a line rather than at a single point by sliding the sensor on the rail. Govignon et al. [8] and Andersson et al. [9] used DSP for the thickness measurement within an area. DSP uses two cameras, separated with a distance, directed to the speckle pattern formed on vacuum bag. With the help of this stereo vision and image processing, the thickness profile of a 2D area can be obtained. The resolution of this type of system depends on the size of the scanned area, and it is found to be ±0.05 mm [8] and ±0.01 mm [9] for the experimented flat panels. To achieve a higher resolution, DSP is not practical, and 3D scanners should be used. Li et al. [3] used a 3D laser digitizer to monitor the thickness of both a flat and 3D composite parts. In this study, laser displacement

sensors will be used. As stated before, the main cause of the thickness variation is the time-varying compaction pressure in the part which is dependent on the resin pressure, P as given in Equation (2). Unlike RTM, the thickness of the mold cavity varies and thus, the porosity of the fabric preform varies with time and spatial coordinates in the VI process. This causes non-uniform permeability of the fabric, which in turn affects the pressure distribution. Modi et al. [10] studied pressure distribution in VI for both linear and radial injections. They observed that, initially, the resin pressure is lower than the corresponding RTM distribution, in which P decreases linearly from the injection gate to the flow front. At later times, the P distribution increased above the RTM distribution. It is stated that, this time-dependent pressure distribution is due to the transient compaction response of the fabric. Moreover, experimental study of Williams et al. [6] presented that compaction of preform consists of (i) an initial and (ii) a time-varying thickness reduction under static loading. These studies support the necessity to include the time-dependent compaction behavior of the preform in the process models. In addition to monitoring of the thickness distribution, Yenilmez et al. [1] and Govignon et al. [8] integrated pressure sensors in their setup to see the coupling effect between pressure and thickness. In this study, a configuration similar to [1] will be used with laser displacement sensors instead of dial gages to eliminate the mechanical contact pressure of sensors.

2.3 Characterization Models

Many preform characterization models are available in the literature and summarized in Yenilmez and Sozer [2,4]. Based on the previous studies, it is shown that wet

and dry compaction/decompaction data and also time-dependent response of fabric compaction must be considered for a realistic and accurate model of the VI process.

Simulations available in the literature use process models based on Darcy law for the resin flow. The permeability, K in Darcy law is dependent on the fiber volume fraction, V_f, hence K is not constant in VI since thickness, h and thus V_f change during resin flow. Most of the models [3,7,11-14] use well accepted Kozeny-Carman equation, $K = A (1 – V_f)^3 / V_f^2$ to fit the experimental data for permeability. Some of the researchers [15,16] preferred power-law fit, $K = a (V_f)^b$. There are also analytical models [17] for an approximated unit cell of geometrically well-defined preforms like woven fabrics. By using Darcy law and the relation between compaction pressure and permeability in the continuity equation, a process model for VI can be obtained. Hammami et al. [11], Park et al. [15] and Joubaud et al. [16] used power-law fit to relate the thickness to the compaction pressure, $h = c P_c^n$. Their model for 1D flow accounts for the nonlinearity of the pressure distribution caused by thickness variation. However, they used a single compaction behavior for both dry and wet regions of the preform, meaning no lubrication effect could be captured. Andersson et al. [12] added a softening term to compaction model to account for the effect of wetting on the compaction. This term decreases the stiffness as the fabric gets saturated, and thus, it gives a more realistic result during the local impregnation. Instead of adding terms to the compaction model, the same effect could be studied by using separate compaction models for dry and wet fabrics. Yenilmez et al. [1] used experimentally collected compaction database for dry and wet fabrics. Their simulation results were compared and verified with experiments. In their following study, Yenilmez et al. [4] included the time-dependent relaxation

characteristics to their compaction model. Govignon et al. [13] used separate power-fit models for dry and wet fabrics. They also included the effect of the compaction history by using interpolations on the data obtained at different relaxation pressures as in [2]. Results of [1], [12] and [13] showed that the lubrication effect upon resin arrival is significant for some types of fabrics, and it should be accounted for a realistic process simulation.

Song and Youn [11] modeled the resin infusion in VI. Resin races through the distribution medium because of its much higher permeability than the bulk preform; and then it saturates bulk preform as it flows in the thickness direction. Utilization of resin distribution media is a cause for the development of the through thickness pressure gradient. Through thickness (transverse) flow, proceeds with in-plane direction flow. As the in-plane direction flow propagates dominantly through the distribution media, transverse flow impregnates preforms simultaneously. Model (both numerical and analytical) and experimental results show variations. Variations are usually because of n models' lack of entirely predicting the effect of the transverse flow.

In their later work, Song and Youn [12] developed a model for the post-infusion stage in VI. Their model examined the resin bleeding. The resin infusion process was modeled with constitutive laws that related permeability of the material and fibre volume fraction, and use a non-linear elastic material equation for compaction; and input data by Correia et al. [10] is used. Three different VI experiments with different settings for bleeding were experimented for the final thickness distribution. In the first experiment, the inlet was closed and the outlet is kept at very low vacuum pressure. The second experiment was a

modification of the first one. The conditions were the same except the outlet was kept at 70 kPa. In the second experiment, the reduced vacuum pressure resulted in an increased part thickness. With the reduced pressure, the equilibrium of the preform pressure and the intra part thickness was reached faster in the first experiment case than in the third experiment,in which “Controlled Atmospheric Pressure Resin Infusion (CAPRI)” procedure was utilized. The inlet was kept at 50 kPa and the outlet at vacuum pressure. With CAPRI process, the initial thickness distribution and thickness variation were reduced. Also the resin waste was minimized (the maximum waste occurs in experiment 1, and the minimum in experiment 2). Experiment 3 had the optimum resin waste while having the highest possible fiber volume fraction after the resin bleeding.

Coupled process models of compaction and resin flow were extended from 1D to 2D in [3,7,14]. Li et al. [3] added compaction and permeability models to an existing RTM process simulation to account for the permeability change due to thickness variation. However, only wet fabric data was used for the compaction model, hence, the thickness values are correct only after the mold filling. Kang et al. [14] used a similar approach, but used modified exponential fit to the compaction data. Kessels et al. [7] used separate power fit for dry and wet fabric. Thus, their model was able to mimic the lubrication effect which significantly changes the thickness values during impregnation.

Heider et al. [16] investigated the effect of the CAPRI process . As stated previously, CAPRI is the abbreviation for Controlled Atmospheric Pressure Resin Infusion. A handful of process steps added to the VI process to achieve a part with reduced thickness variation.

These steps were included in three stages of the VI process which were Material preparation, Infusion step, and Post-Infusion steps. In material preparation step, the resin was subjected to vacuum pressure. As a result, the resin was dried off moisture and other additives which may form voids in the part structure. Another important step for the material preparation was pre-infusion debulking. Pre-infusion debulking is the repeated compression-relaxation cycles applied on of the preform. Using debulking,they could have reduced the 0.4mm part thickness variation to 0.25mm. 5% decrease in total thickness with a 5% increase in fiber volume fraction was also noted to appear as a result of debulking. In the injection stage, full vacuum was applied to the ventilation gate. Apart from an ordinary VI process, the injection gate was subjected to a half vacuum. The half vacuum applied to the injection gate decreased the absolute pressure difference within the system, and thus decreased the pressure gradient as well. Four experiments were conducted for comparison. These were full vacuum, full vacuum with debulking, half vacuum, and half vacuum with debulking. Debulking decreased the overall thickness of the part as well as thickness gradient. After the injection stage, full vacuum experiment had the highest thickness difference of the four experiments. For the full vacuum experiment, the thickness was between 8.5 mm and 8.2 mm. Using half vacuum decreased the thickness gradient significantly compared to full vacuum (the thickness of the intra part was between 8.3 mm and 8.2 mm for half vacuum case). Use of debulking in full vacuum and half vacuum experiments decreased overall part thickness and thickness variation. The debulking is the major factor affecting the thickness gradient. As a result, experiments conducted with debulking had similar thickness varying around 7.8 mm for both half vacuum and full vacuum

cases. Experimental results by Heider et al. showed that debulking reduced the spring back effect of the preform as much as 40%. As a result, reduced thickness variation was observed after full injection.

2.4 Objective

The objective of this study is to achieve the reduction of the part thickness variation hence, to obtain a uniform thickness along the part by developing an injection control procedure in the VI process. The compaction and decompaction databases formed in [2], and pressure distribution model for a particular mold cavity were used to control the process. Various control actions include:

- opening additional ports for ventilation or injection,
- varying ports' pressures,
- bleeding excess resin at the end.

The main purpose of these actions and experiments is to create a methodology of minimization of thickness variation for VI applications.

CHAPTER 3

1D EXPERIMENTS

3.1 Experimental Setup

The vacuum infusion setup is shown in Figure 1. The rigid mold plate consists of three multifunctional ports, seven piezoelectric pressure transducers (shown as P_{in}, P_1, P_2,…, P_5, P_{exit}), five thickness sensors (H_1,H_2,…,H_5) and three reservoirs/traps with internal scales. The pressure transducers' (Microsensor MPM280) range is 0-100 kPa with an accuracy of ±0.3 kPa. There are three multifunctional ports; any one of them can be used as either an injection gate (resin inlet) or a ventilation port (air and resin exit).

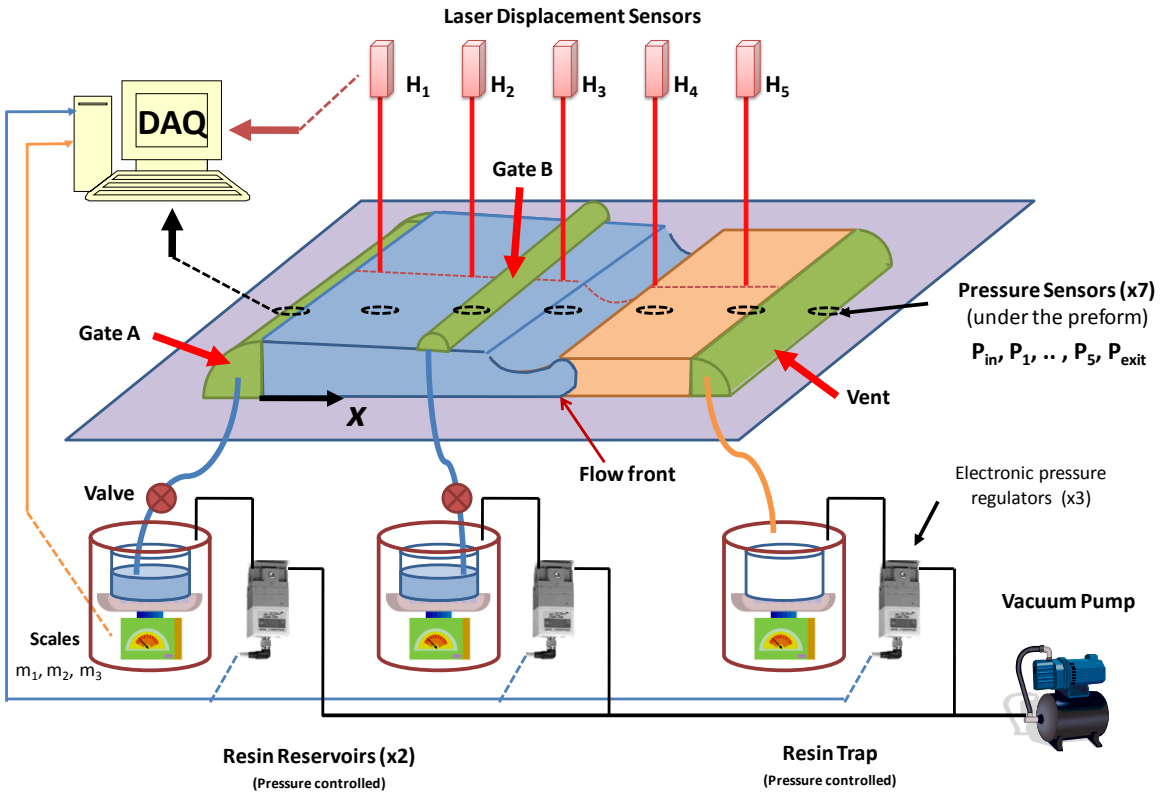

Figure 1 Experimental setup. The displacement sensors H_1, H_2,…, H_5 and the pressure sensors P_1, P_2,…, P_5 are located at x = 20, 80, 140, 200, 260 mm; the fabric preform has a length of 280 mm in the x direction.

The experimental setup configuration shown in Figure 1 has the two ports being used as injection gates and the right port is used as a ventilation port. Each of these ports is connected to a separate pressure controlled resin reservoir/trap. The scales inside the reservoirs and the trap are used to measure the resin mass. An injection gate can be closed at a particular time, it may be converted to a ventilation port on-line; or just the opposite control action can be done (i.e., a ventilation port can be converted to an injection gate) according to the control action schedule which can be determined by each experiment's

data acquisition and evaluation. The vacuum is obtained using a vacuum pump (Alcatel Pascal 2010 SD). To draw different levels of vacuum at different locations of the mold and adjust the inlet resin pressure, the vacuum pump is connected to resin reservoir/trap(s) through SMC ITV2090 electronic vacuum regulators. Above the mold, there are five Omron Z4M-W40 laser displacement sensors (shown as $H_1, H_2,\ldots, H_5$) which have a resolution of 1.5 µm, and they are used to measure the thickness of the preform at the same x locations of the pressure sensors, $P_1, P_2,\ldots, P_5$. The scales, vacuum regulators, pressure sensors and laser displacement sensors are all connected to an NI PCI-6035E data acquisition card, which allows monitoring and recording of all the pressure, thickness and mass data.

The preparation of the experiment begins with coating a very thin film of release wax and then placing the reinforcing fabric preform on the mold. The preform consists of eight layers of Fibroteks e-glass random fabric (500 g/m^2 per layer), and one layer of Metyx Meticore 250PP core material (made of polypropylene; 250 g/m^2) placed in the middle of the random fabric layers like a sandwich. The in-plane dimensions of the preform are 280 mm x 100 mm. The fabric preform is covered with a peel-ply for easy removal of the disposable materials after the mold filling and resin cure. To create a linear injection, omega tubes and flow meshes (a.k.a. distribution medium) are placed at the injection and ventilation ports. The vacuum bag is placed over the peel-ply and secured to the mold with a tacky tape to seal the mold cavity. The vacuum is started and the system is checked for possible air leaks. After the desired level of vacuum is achieved, the computer starts recording pressure, thickness and mass data. After 15 minutes of initial vacuuming, the resin is prepared by adding 0.007% cobalt and 1.0% MEK peroxide (by weight) to Poliya^{TM} Polipol 337 polyester in order to start curing (cross-linking) reaction. The gelation time (a.k.a. pot

life) can be set by adjusting the additive ratios, and at the mentioned ratio, it is approximately 35 minutes at room temperature. When the resin is ready, the injection is started. The data acquisition continues until the demolding of the composite part. Labview control panel allows the user to monitor and adjust the process parameters for on-line control actions.

Repetitive experiments have been done to show the effect of control actions [19]. Results of one of the experiments will be presented together with an uncontrolled experiment for comparison. The uncontrolled experiment will be called Case A, and the controlled experiment will be called Case B.

3.2. Case A: VI Experiment with No Control Action but Only Bleeding of Resin During Post-Mold Filling

In Case A, a VI experiment will be conducted without any control action to show the typical thickness variation in a composite part. It is expected to have a thickness distribution which is maximum at the inlet due to low compaction pressure, and minimum at the outlet due to high compaction pressure.

Since it is known that the pressure variation is the main cause of the thickness variation, bleeding of the excess resin can be done to reduce this, as also studied in [14]. After the complete mold filling, the inlet gate is closed, thus the pressure inside the mold starts to equalize. As a result, the overall thickness variation decreases. However, as explained before, the fabric may, and usually will, have a time dependent compaction behavior based on the compaction/decompaction history [2]. In that case, even if the final

pressure is constant everywhere in the fabric preform, the thickness distribution may have a variation with time due to different compaction/decompaction histories of different locations. For example, the points closer to the inlet remains under a very low compaction pressure during mold filling; on the other hand, the points closer to the outlet remains under the maximum level of compaction since the resin pressure is the lowest there. Hence, the thickness variation cannot be completely eliminated with only bleeding, but can be kept within a tolerance if appropriate control actions are taken, as will be illustrated in Case B.

The results of Case A are shown in Figures 2 and 3. Horizontal axis is the non-dimensional time, , where t_{MF} is the mold filling time. In these figures, black vertical lines denote the resin arrival times to the sensor locations 1 to 5 (t^*_{S1} to t^*_{S5}) as well as the mold filling time (t^*_{MF}). Figure 2 shows the resin pressures measured by P_{in}, P_1,…, P_5 and P_{exit}. The inlet pressure was 8 kPa lower than the atmospheric pressure. It is due to the elevation difference of 75 cm between the resin reservoir and the mold, thus $\Delta P = P_{atm} - P_{in} = \rho_{resin}\, g\, h$ = (1.096 kg/m^3)(9.81 m/s^2)(0.75 m) = 8 kPa. At an instant, say at the time of mold filling ($t^* = 1.00$), the resin pressure decreases almost linearly along the *x* direction. *P* would be a perfect linear function of *x* (with a constant slope) if the mold cavity had a constant thickness as in the RTM application, however here in the VI process the thickness is not constant and thus the deviation from the linearity is not surprising (see Figure 4). At $t^* = 1.40$, the inlet was closed and the excess resin in the thicker regions of the fabric was forced to bleed out. The pressure inside the mold started to decrease down to the vacuum pressure during the bleeding stage. Notice that the conventional bleeding application uses a bleeder material above the peel-ply and the resin flow occurs mainly in the thickness direction. However, in

this study, bleeding was applied simply by letting the excess resin flow in the *x* direction and exit from the vent due to the unconventional placement of the distribution medium.

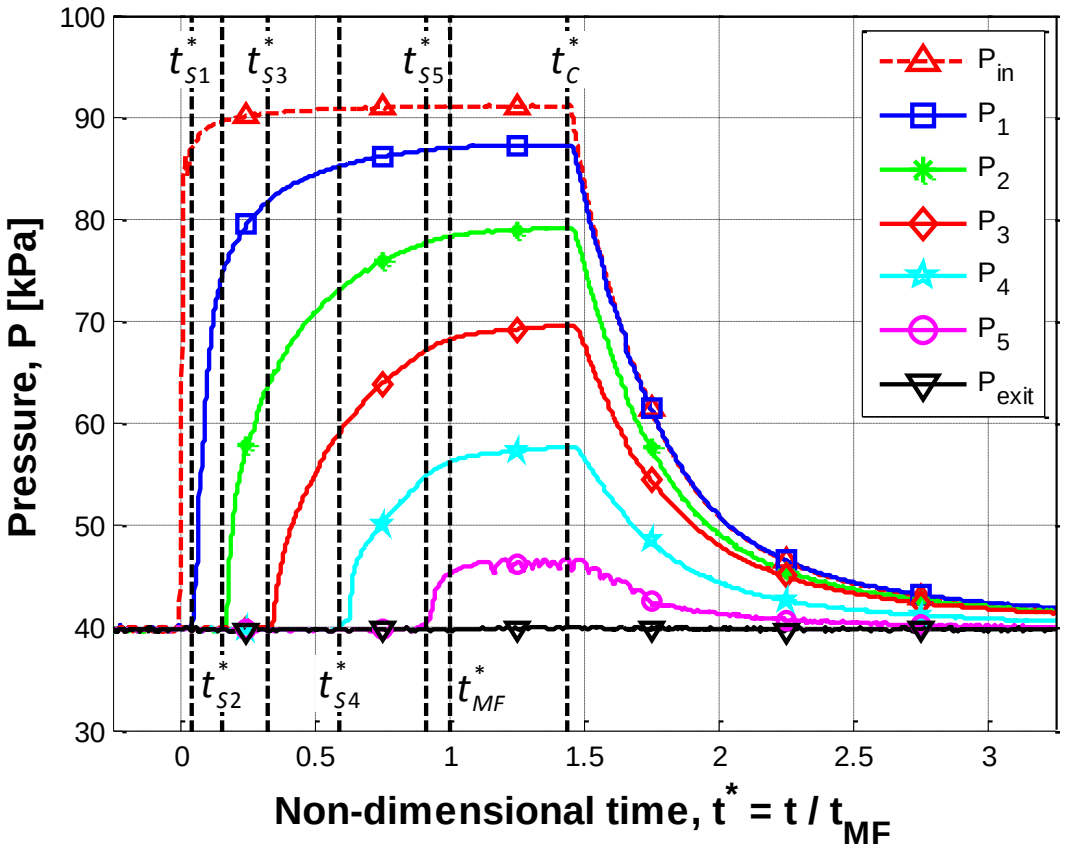

Figure 2 Experimental resin pressure for Case A. t_{Si} is the resin arrival time to sensor *i*, and t_C is the time of the control action.

The change in thickness ΔH can be seen in Figure 3 at the five sensor locations as a function of time. ΔH is defined as $\Delta H \equiv H(x,t) - H(x,0)$ where $H(x,t)$ and $H(x,0)$ are the instantaneous and initial thicknesses, respectively. The lubrication effect can be clearly seen in this random type of fabric, which was previously observed in [1,2]. As the resin reaches a sensor location, the fabric preform compacts even more before it expands in spite of the decrease in the compaction pressure decreases. At the sensor locations near the inlet,

increase in the thickness is higher than the sensors away from the inlet due to the lower compaction pressure near the inlet than the exit. After the complete mold filling, sensor pressure values stayed almost constant but the thicknesses continued to change, which supported the fabric's time-dependent behavior as also seen in [2] for this particular preform. This increase in thickness continued until the injection gate was closed for bleeding and thus the compaction pressure started increasing. After the injection gate was closed, the thicknesses started decreasing with a decreasing rate. The thickness variation was decreased, but not eliminated completely.

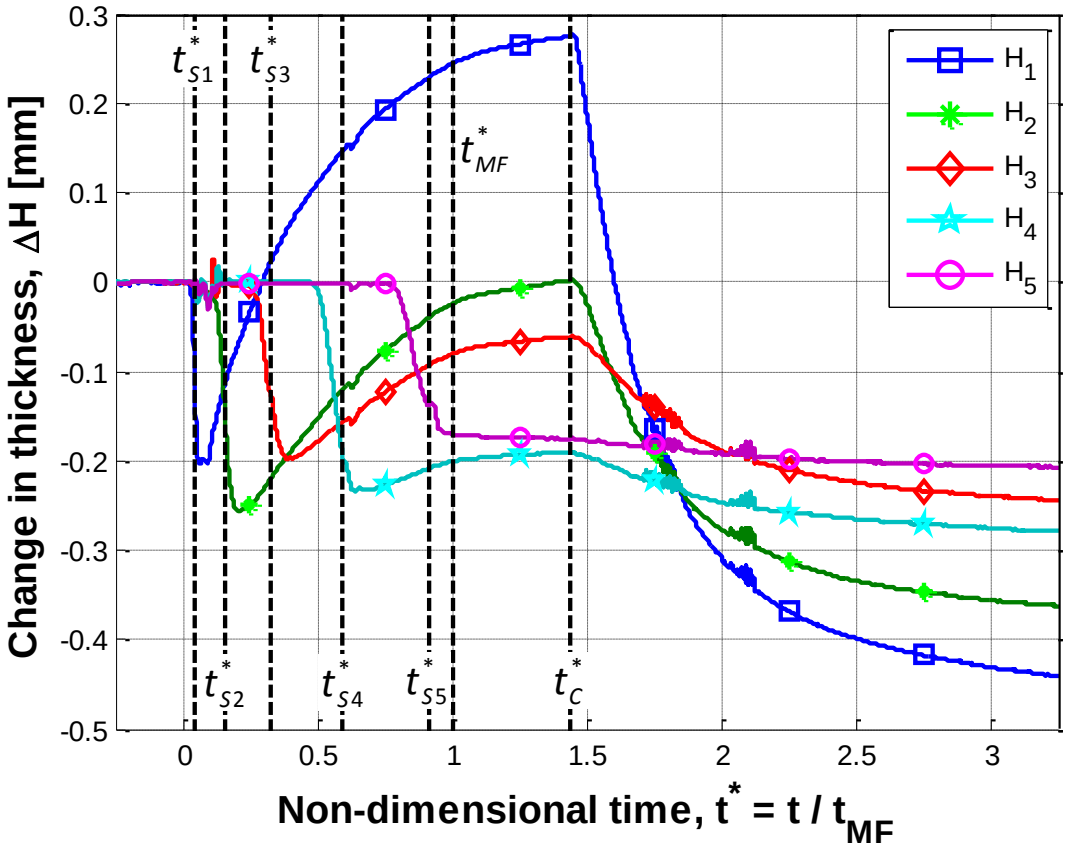

Figure 3 Change in thickness, $\Delta H \equiv H(x,t) - H(x,0)$ for Case A. t_{Si} is the resin arrival time to sensor *i*, and t_C is the time of the control action.

The maximum percentage of thickness variation at a particular time *t*, is calculated as:

$$\Delta H_{\text{var}}(t) = \frac{[H(x,t) - h(x,0)]_{\max} - [H(x,t) - H(x,0)]_{\min}}{[H(x,t)]_{average}}. \qquad (3)$$

It was calculated that the thickness variations are $\Delta H_{\text{var}}(t_{gelation}) = ([-0.22] - [-0.47])/5.04 = 0.0496 = 4.96\%$ at gelation, and $\Delta H_{\text{var}}(t_{gelation} + 30\text{min}) = ([-0.29] - [-0.56])/4.96 = 0.0544 = 5.44\%$ 30 minutes after the gelation.

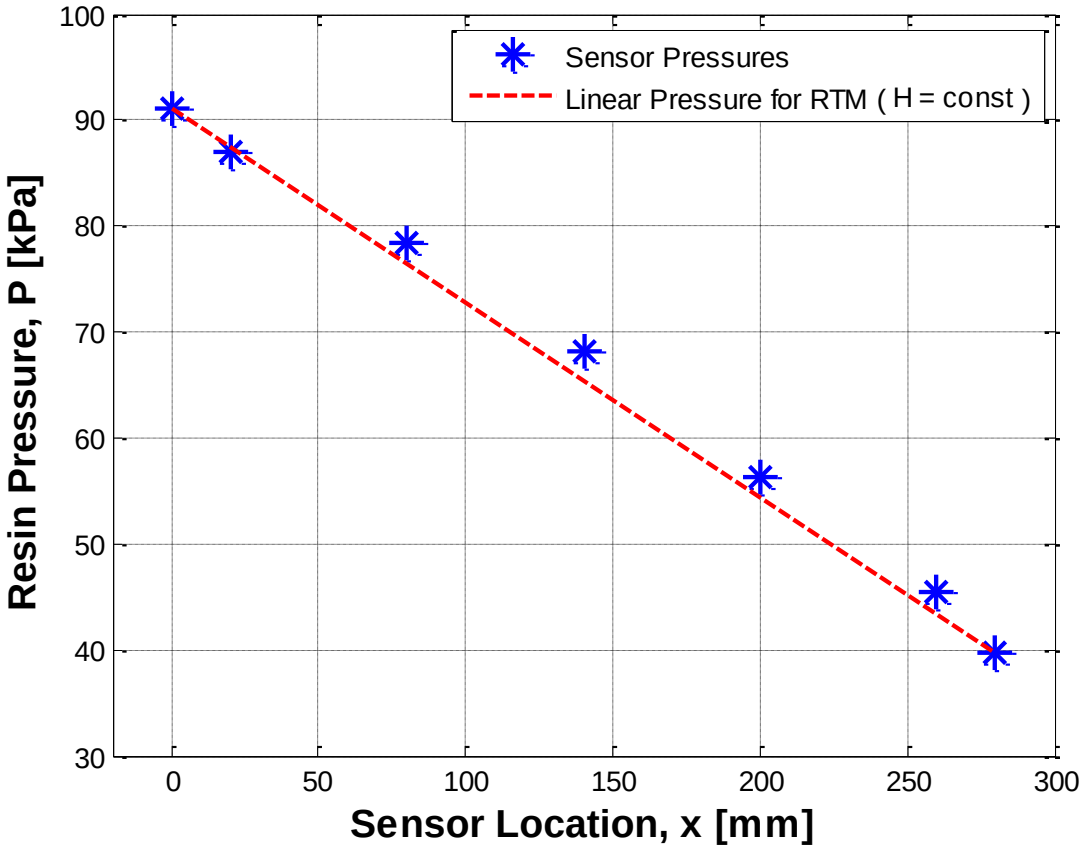

Figure 4 Experimental resin pressure distribution at the time of complete mold filling (t* = 1) for Case A. $P(x,t_{MF})$ deviates slightly from the linear pressure distribution corresponding to *h* = constant case in RTM.

3.3. CASE B: Experiment with Control Actions

In Case B, control actions were applied after the mold was filled completely to decrease the thickness variation. During the mold filling, the same inlet and outlet gates were used as in Case A, but an additional gate was introduced to the system after the mold filling. The additional gate, Gate B was located at x = 170 mm (in the middle of Sensors 3 and 4). Control actions were decided before the experiment based on the results obtained from Case A and knowing the compaction/decompaction characteristics of the fabric and core types used in this study as previously studied in [2]. The infusion parameters of Case B are the same as in Case A during the mold filling. The control actions are tabulated in Table 1 and detailed below.

Table 1: Control actions taken in Case B.

Action #	Non-dimensional Time, $t^* = t/t_{MF}$	Gate A Pressure, P_{in} [kPa]	Gate B Pressure [kPa]	Vent Pressure, P_{exit} [kPa]	Actions	Expected Results
0	0	100	X	40	Injection is started with Gate A and the vent are open, and Gate B is kept closed.	1D resin injection (from left to right).
1	1.20	20	60	40	Gate B is activated with a pressure of 60 kPa (just before Action #1, the pressure at that location was interpolated as ~60 kPa) and Gate A's pressure was decreased to 20 kPa.	Reverse the direction of flow between Gates A and B (from right to left).
2	1.80	60	50	40	Gate A's pressure was increased to 60 kPa, and B's pressure was decreased to 50 kPa.	Reverse the direction of flow between Gates A and B (from left to right). This is similar to Action #0, except that, it should allow a higher compaction near the inlet.
3	2.20	X	X	40	Gate A and B are closed.	The excess resin is forced to bleed out.

"X" means the gate is closed.

t_{MF} denotes the time of complete mold filling, and it is approximately 300 seconds in this experiment

- Control Action 1: It took place 1 minute after the complete mold filling ($t^* = 1.20$). Gate B was opened and its reservoir pressure was set to 60 kPa, which kept the pressure distribution between Gate B and the outlet unaffected (by knowing the resin pressure at that location from Case A). At the same instant, Gate A pressure, P_{in} was decreased to 20 kPa. This is expected to change the direction of resin flow: from Gate B to Gate A, whereas the resin flow was from Gate A toward left initially. More importantly, as the resin pressure was decreased and thus, the compaction pressure was increased near Gate A, the thickness was expected to start decreasing in this previously relaxed region.

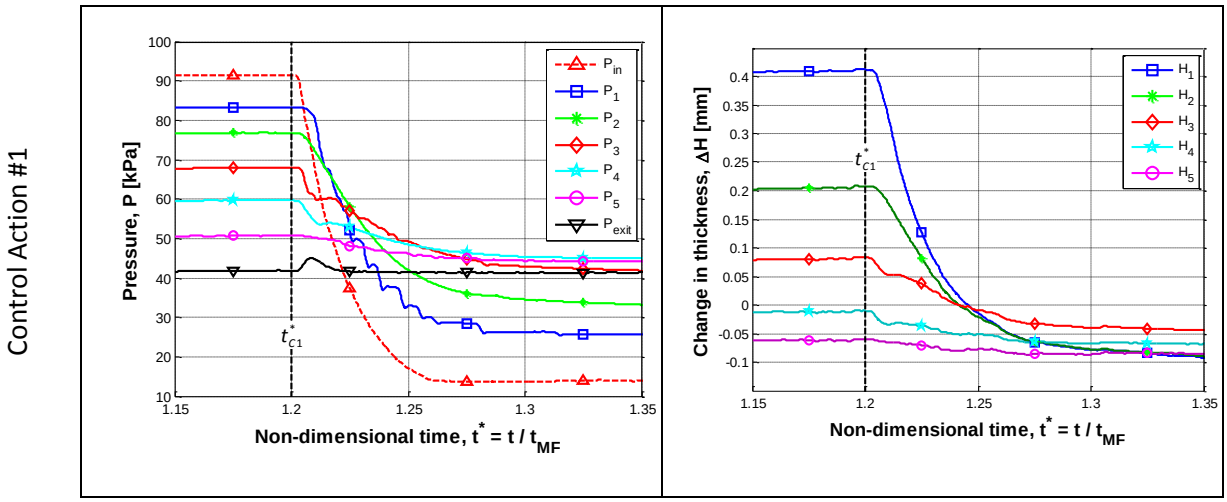

Figure 5 Post filling result of Case B for control action 1: **pressure variations, P(t)** (left) and **thickness variations, h(t)** (right), $t_{C1}^{*} = t_{C1} / t_{MF} = 1.20$

- Control Action 2: It took place 4 minutes after the mold filling ($t^* = 1.80$). This control action reversed the resin flow once again between Gates A and B, and this way, an excess compaction of the fabric preform near Gate A was avoided by increasing the resin pressure and thus, decreasing the compaction pressure there compared to the rest of the preform.

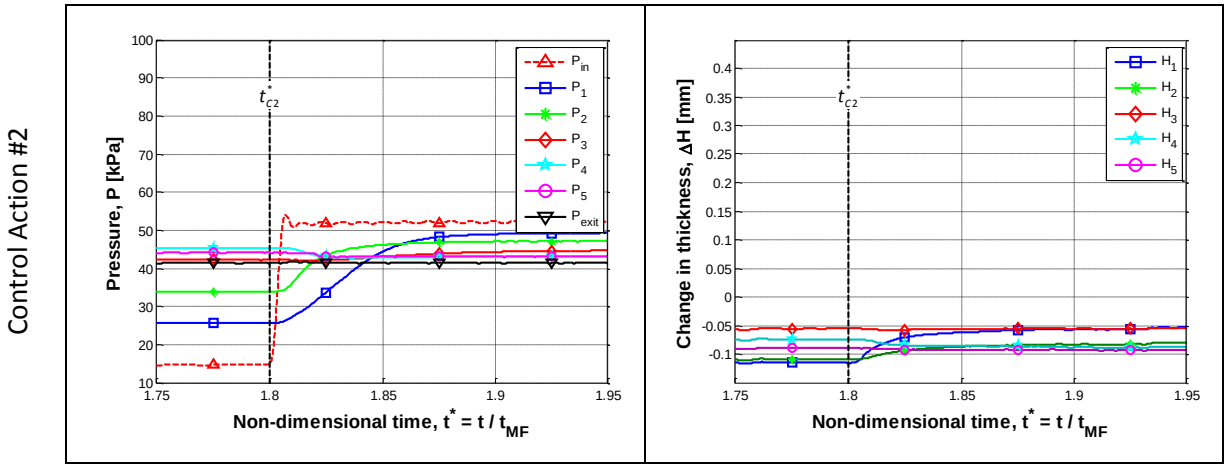

Figure 6 Post filling result of Case B for control action 2: **pressure variations, P(t)** (left) and **thickness variations, h(t)** (right), $t_{C1}^{\ *} = t_{C1} / t_{MF} = 1.80$

- Control Action 3: It was done at $t^* = 2.20$ to bleed the excess resin out of the thicker regions of the preform, as also done in Case A. The difference from Case A was that, more uniform compaction history was expected to be achieved due to Control Action 1, thus, it was expected to result in much less thickness variation in this Case B than Case A.

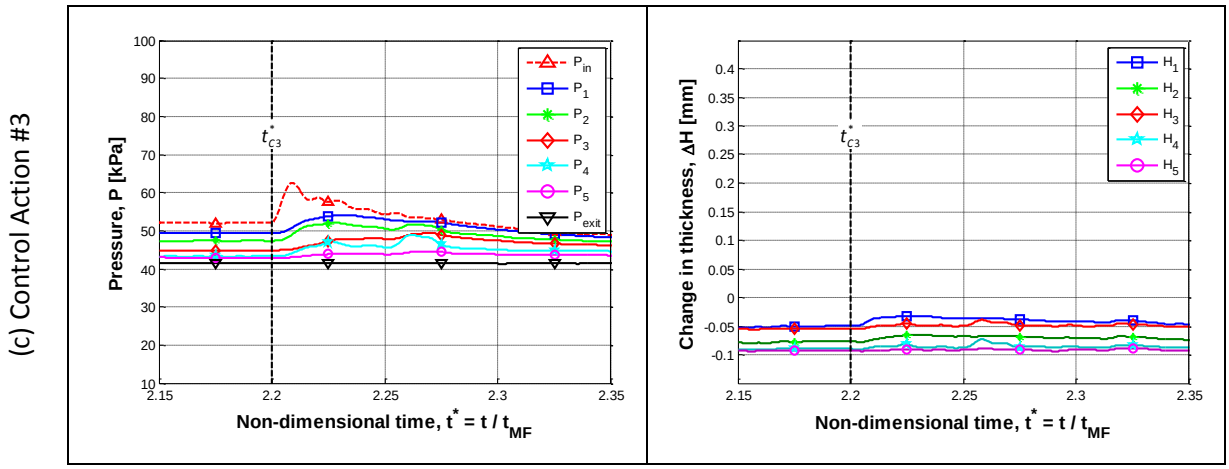

Figure 7 Post filling result of Case B for control action 3: **pressure variations, P(t)** (left) and **thickness variations, h(t)** (right), $t_{C1}^{*} = t_{C1} / t_{MF} = 2.20$

The experimental results of Case B are shown in Figures 5 - 9. Similar to the results of Case A (shown in Figures 2 and 3), the vertical black lines indicate the resin arrival times to the sensors locations, the time of complete mold filling and time of control actions ($t_{C1}^{*}, t_{C2}^{*}, t_{C3}^{*}$) in Figures 8 and 9. Overall pressure and thickness changes can be seen in Figures 8 and 9, respectively.

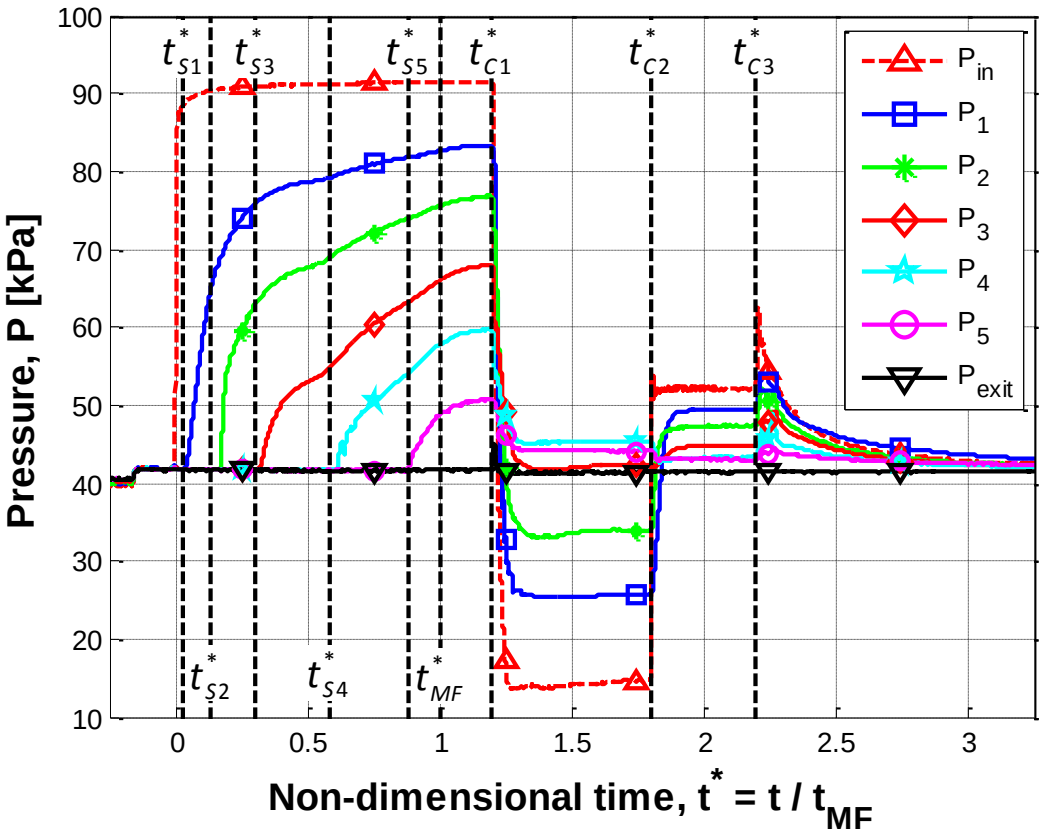

Figure 8 Experimental resin pressure for Case B. t_{Si} is the resin arrival time to sensor *i*, and t_{Cj} is the time of the control action *j*.

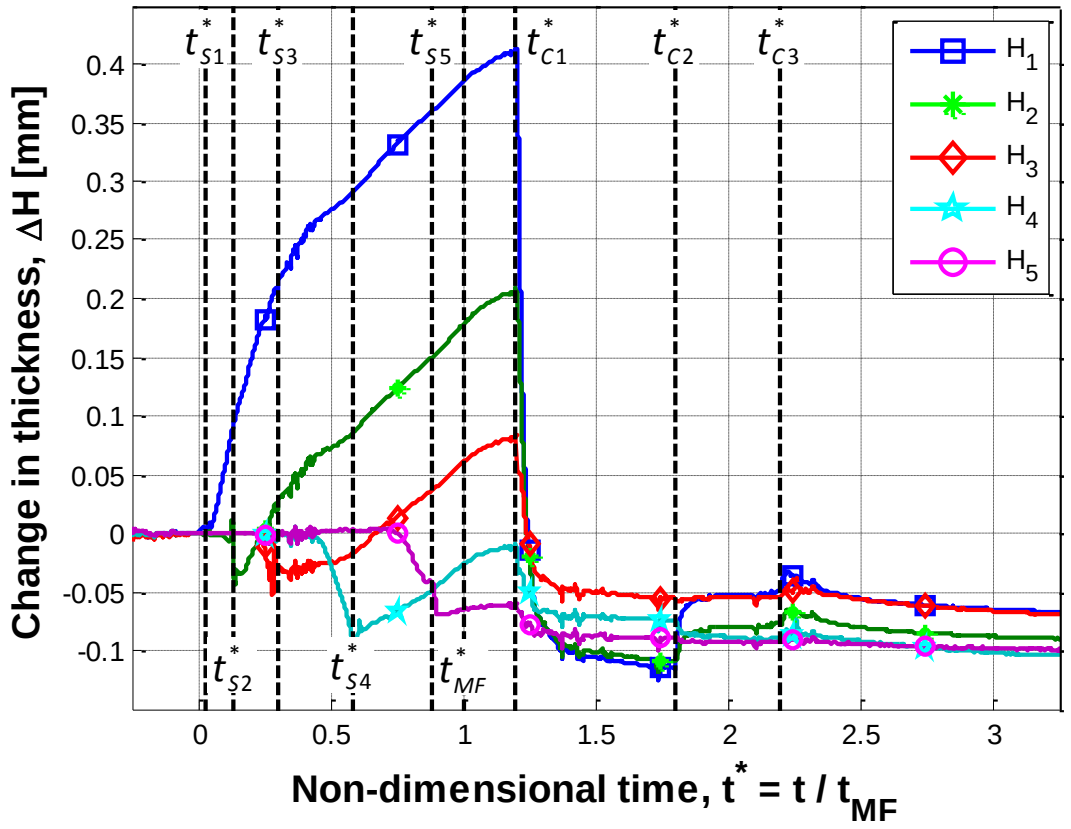

Figure 9 Change in thickness, $\Delta H \equiv H(x,t) - H(x,0)$ for Case A. t_{Si} is the resin arrival time to sensor *i*, and t_{Cj} is the time of the control action *j*.

Mold filling was observed at $t = t_{MF}$ = 300 s approximately ($t^* = 1.00$). The effects of the first control action, which was executed at t = 360 s ($t^*_{C1} = 1.20$), can be seen in Figures 4 and 5. The fabric preform responded to the change in pressure rapidly by being further compacted at the first three sensor locations. The variation in thickness continued decreasing for the next 3 minutes. The second control action was executed at t = 540 s ($t^*_{C1} = 1.80$); and it caused the fabric to relax near Gate A. The thickness increased at the first two sensor locations; and the maximum thickness variation decreased as clearly seen from Figure 7. The bleeding was applied as the last control action at t = 660 s ($t^*_{C1} = 2.20$). Both

Gates A and B were closed by bending and clamping the injection tubes. During this action, small pressure fluctuation was observed which also affected the thickness for a while. At this final stage, the pressure was equalized inside the mold cavity, and the fabric continued to compact at a slow pace until the resin gelation due to time-dependent fiber settling/relaxation characteristics of the preform.

At $t = t_{gelation}$ + 30 minutes, $\Delta H_1(t)$ was measured as -0.12 mm by the first sensor, and the rest of the sensors measured $\Delta H_2,\ldots,\Delta H_5$ as -0.14 mm each. This indicated the maximum variation in the composite part as $\Delta h_{\text{var}}(t_{gelation}+30\text{min}) = ([-0.12]-[-0.14])/5.10 = 0.0039 = 0.39\%$ Compared to Case A, where no control action was taken other than bleeding; a better job has been done here by decreasing the maximum thickness variation from 5.44 % to 0.39 %.

Experiments with a flow mesh are also conducted. These experiments are explained in Appendix B.

CHAPTER 4

2D EXPERIMENTS

In a conventional VI process,no action is taken after mold filling, and the part is de-molded after partial or complete resin cure. A usually common practice is the bleeding process, which is the closure of the inlet tubing so that the excess resin will be bled through the outlet. Bleeding is used to increase fiber volume fraction (V_f) and also to decrease the part's thickness variation. However, as studied in [2] even after 15 minutes of bleeding, a VI part cannot reach an insignificant thickness variation. In this paper, in addition to bleeding, a set of pre-defined control actions (based on compaction database of the fabric preform used) will be used to further decrease thickness variation. The term "control action" is used for activities (adjustment of process parameters) performed on the setup after mold fill. These activities encompass (1) introducing multi-purpose ports (which can be used either as an injection gate or as a ventilation port) to the system, (2) changing the pressure of the existing gates and ports, (3) closing existing gates and ports, and (4) bleeding of excess resin through vent.

4.1 Process Modeling

As previously mentioned, a relatively crude shape (resembling a crude F) is selected as a case study here. Four different multi-purpose port locations are selected along the edges of this shape. The locations of multi-purpose ports have been chosen, by considering the results of a compaction model. Using finite differences, the pressure distribution inside the mold cavity is calculated. Figure 12 shows the discretized domain for the F shaped part, the governing differential equation for P, and boundary conditions. Using Darcy's law for flow through a porous medium substituted in the conservation of mass, one can obtain the governing equation for inner points:

$$K_{xx}\frac{\partial^2 P}{\partial x^2} + K_{yy}\frac{\partial^2 P}{\partial y^2} = 0 \qquad (4)$$

where $K_{xx\ and}$ K_{yy} are permeability components along x-, and y-axes, and P is liquid resin pressure. Discretization of Equation (4) results in

$$\frac{\partial^2 P}{\partial x^2} = \frac{1}{h_x^2}\left[P_W - 2P_C + P_E\right] + O(h_x^2) \qquad (5)$$

$$\frac{\partial^2 P}{\partial y^2} = \frac{1}{h_y^2}\left[P_N - 2P_C + P_S\right] + O(h_Y^2) \qquad (6)$$

where P_c is the central pressure at point (i,j), P_N is the North pressure at point (i,j+1), P_S is the South pressure at point (i,j-1), P_W is the West pressure at point (i-1,j), P_E is the East pressure point (i+1,j). Central finite difference is used for Equations (5) and (6) as shown in Figure 13

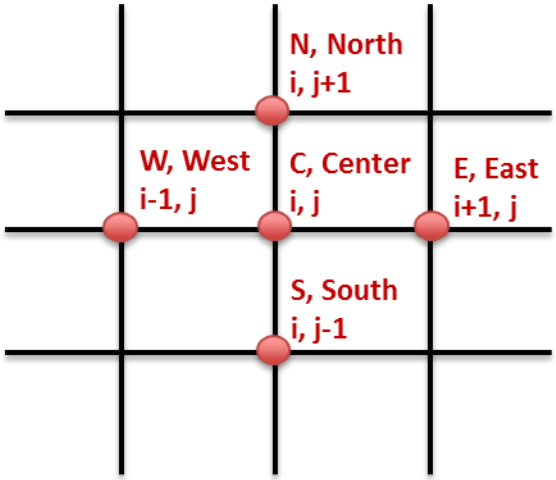

Figure 10 Central finite differences stencil used for Equations (5) and (6)

$$\left(\frac{\partial P}{\partial x}\right)=\frac{-3P_{1,j}+4P_{2,j}-P_{3,j}}{2h_x}=0 \tag{7}$$

$$\left(\frac{\partial P}{\partial y}\right)=\frac{-3P_{i,1}+4P_{i,2}-P_{i,3}}{2h_y}=0 \tag{8}$$

where $h_{x \text{ and }} h_y$ are the increment lengths along x, and y-axes. The stencil used for left edge of the mold is shown in Figure 14:

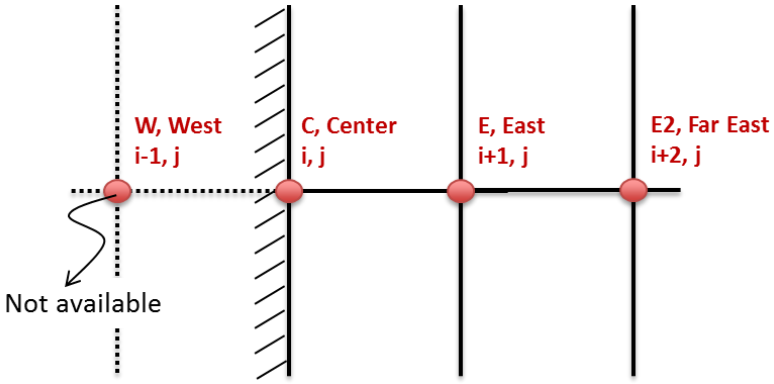

Figure 11 Stencil of one-sided finite differences used for the left edge of the mold. Due to the absence of West point, forward finite difference will be applied instead of a central difference.

After calculating pressure field, compaction database obtained from [3] is used to calculate thickness of the preform. From compaction database, a point's thickness value can be estimated for the calculated pressure affecting it considering an elastic compaction model. As a validation check case, total inflow and outflow are calculated to check if the model correctly calculates the pressure field. If the calculated inflow is equal to the calculated outflow (within the accuracy of numerical method), then the global conservation of mass is satisfied; and the model is assumed to work correctly.

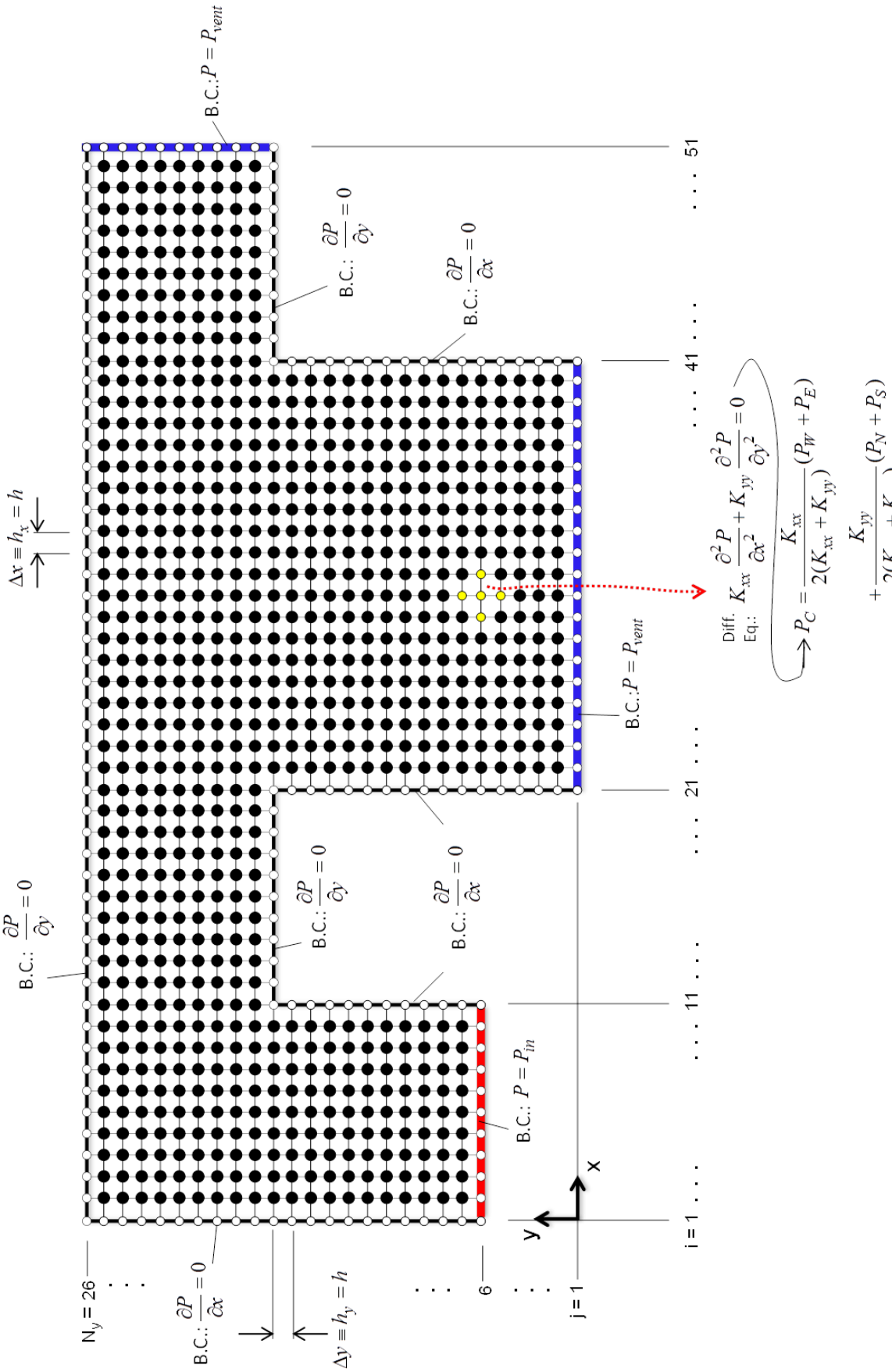

Figure 12 The discretized domain, governing differential equation for P, and boundary conditions.

4.2 Selection of Control Actions

The effect of boundary conditions (pressure magnitude on multi-purpose port locations) is investigated here. In the experimental setup, pressures at multi-purpose ports are controlled via regulators. By changing the pressure, the multi-purpose ports can be used as either (i) an injection gate or (ii) a ventilation port. Different multi-purpose gate locations selected for this case study are shown in Figure 16.

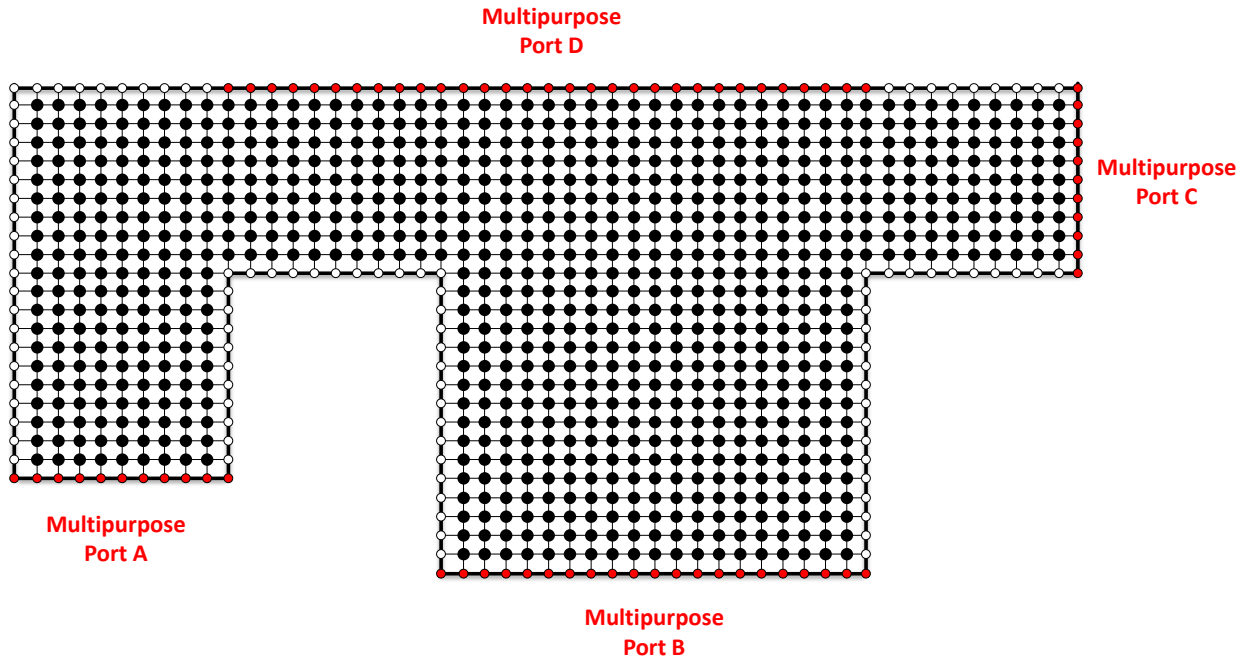

Figure 13 Locations of multi-purpose ports

For these four port locations, three different pressure values (100 kPa (an inlet open to atmosphere), 40kPa, 20kPa) have been investigated using the FDM method. Mean thickness values h_{mean}, maximum thickness values h_{max}, minimum thickness values h_{min}, percent thickness variation Δh_{var}, and standard deviation σ, are calculated for each combination and are tabulated on Table 1. Δh_{var} is calculated using:

$$\Delta h_{\text{var}} = \frac{\left[h(x,y,t) - h(x,y,0)\right]_{\max} - \left[h(x,y,t) - h(x,y,0)\right]_{\min}}{\left[h(x,y,t)_{average}\right]} \tag{9}$$

whereis the maximum change in thickness, is the minimum change in thickness and is the average thickness and standard deviation σ is calculated using:

$$\sigma = \left[\frac{1}{n-1}\sum_{i=1}^{n}\left(h(x,y)_i - h^2(x,y)_{average}\right)\right]^{\frac{1}{2}} \tag{10}$$

where n is the total number of points, $h(x,y)_i$ is the thickness of a random point and $h(x,y)_{average}$ is the average thickness.

For experiments, control actions providing the lowest standard deviation is selected. It should be noted that the code assumes an elastic compaction model, i.e., it does not take into account viscous behavior of the composites. Case 9 in Table 2 presents 25.5 % thickness variation and it is the lowest among other investigated cases. The second and third lowest thickness variations, Δhvar, with values of 26.1% and 27.2%, occurred in Cases are 10 and 4, respectively. However, one may object to this conclusion saying that Cases 9 and 10 are basically alost equivalent since thay use the same port combination (except that PA = 20 kPa in Case 10 whereas it was 40 kPa in Case 9), therefore one may not consider Case 10 as a separate case study.

Table 2: Pressure values for multi-purpose ports and their effects on mean thickness h_{mean}, maximum thickness h_{max}, minimum thickness h_{min}, percent thickness variation Δh_{var}, and standard deviation σ.

Case #	P_A (kPa)	P_B (kPa)	P_C (kPa)	P_D (kPa)	h_{mean} (mm)	h_{max} (mm)	h_{min} (mm)	Δh_{var} (%)	σ (mm)	The Order of Least Δh_{var}
1	100	X	40	X	3.82	4.73	3.67	27.7	0.109	4
2	100	X	20	X	3.77	4.73	3.66	28.3	0.119	7
3	100	X	X	40	3.72	4.73	3.67	28.5	0.126	8
4	100	100	100	40	3.90	4.73	3.67	27.2	0.140	3
5	100	100	100	20	3.85	4.73	3.66	27.8	0.137	5
6	100	X	X	20	3.70	4.73	3.66	28.8	0.123	9
7	100	40	40	X	3.78	4.73	3.67	28.1	0.117	6
8	100	20	20	X	3.74	4.73	3.66	28.5	0.124	8
9	40	100	X	100	4.15	4.73	3.67	25.5	0.103	1
10	20	100	X	100	4.09	4.73	3.66	26.1	0.120	2

4.3. Experimental Setup

4.3.1 Measurement Hardware

The experimental setup is shown in Figure 18. A galvanized iron of 3 mm thickness with the dimensions of 1200 mm to 760 mm is used as the lower mold. A thickness scanning setup was built for this study to monitor the thickness distribution in the fabric preform. Two LSK 25-RAY rails, (one 1200 mm, and the other is 1000 mm; this difference is due to the necessity of a space for the motor used), are mounted to the lower mold. On each rail, two LSK GL 25 CA tracks are placed. Since the

driving force will be applied only from one of the rails, two tracks on each rails is used to increase the stability. A Leadshine 57HS22 hybrid stepping motor is used for the motion along the x-axis direction. A platform is mounted on the four tracks. On the platform, a similar mechanical system is mounted for the motion along the y-axis. One Omron Z4M-W40 laser displacement sensor, with a resolution of 1.5 μm, is assembled to this platform. The motor has 400 steps per revolution at a half-step and the pitch length of the timing belt is 5 mm. The timing belt is connected to a pulley with 30 teeth. The motor was connected in a bipolar configuration. The maximum torque that can be obtained by the stepper motor is 1.5 Nm. The precision of the system is calculated as follows:

$$\text{Precision} = \frac{\text{Pitch length of timing bolt x Pulley's teeth number}}{\text{Number of step per revolution}} = \frac{5 \times 30}{400} = 0.375 \text{ mm} \qquad (11)$$

This means that the precision of x in h(x,t) is 0.375 mm when the scanner reads h at a particular x location.

In the experiments, the laser sensor collects data along x-axis. Once the moving tray reaches the limit x-axis, it moves in y-axis in a small increment without collecting data. After the laser sensor is in the desired position along y-axis, it starts moving (and collecting data) along x-axis until the other end. The complete scanning of the mold takes 29 seconds; and the path of the sensor during a full cycle is given in Figure 17:

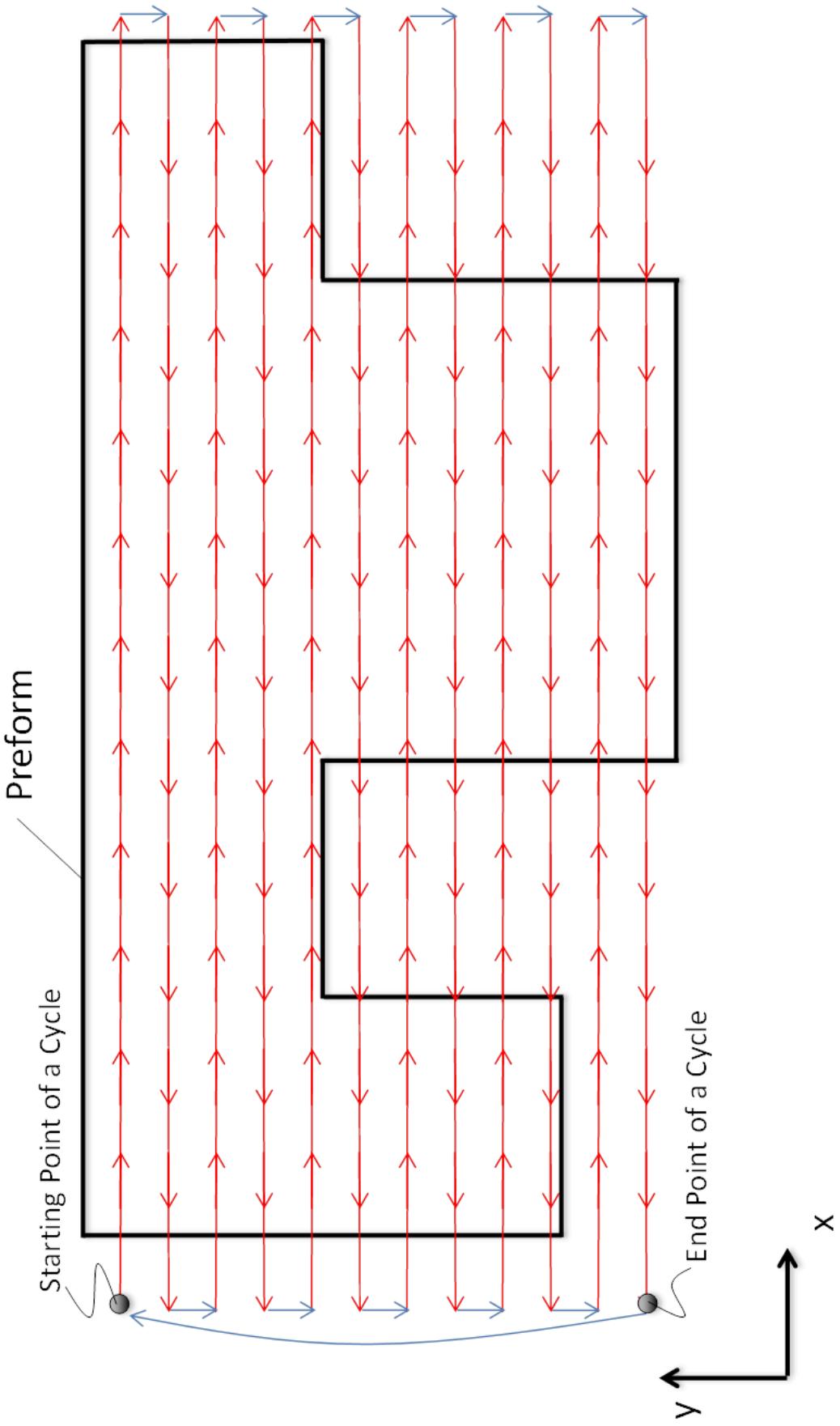

Figure 14 The path of the scanning sensor during a full cycle. Red arrows denote the paths of the movement along x-axis, and blue arrows denote the paths of the movement along y-axis.

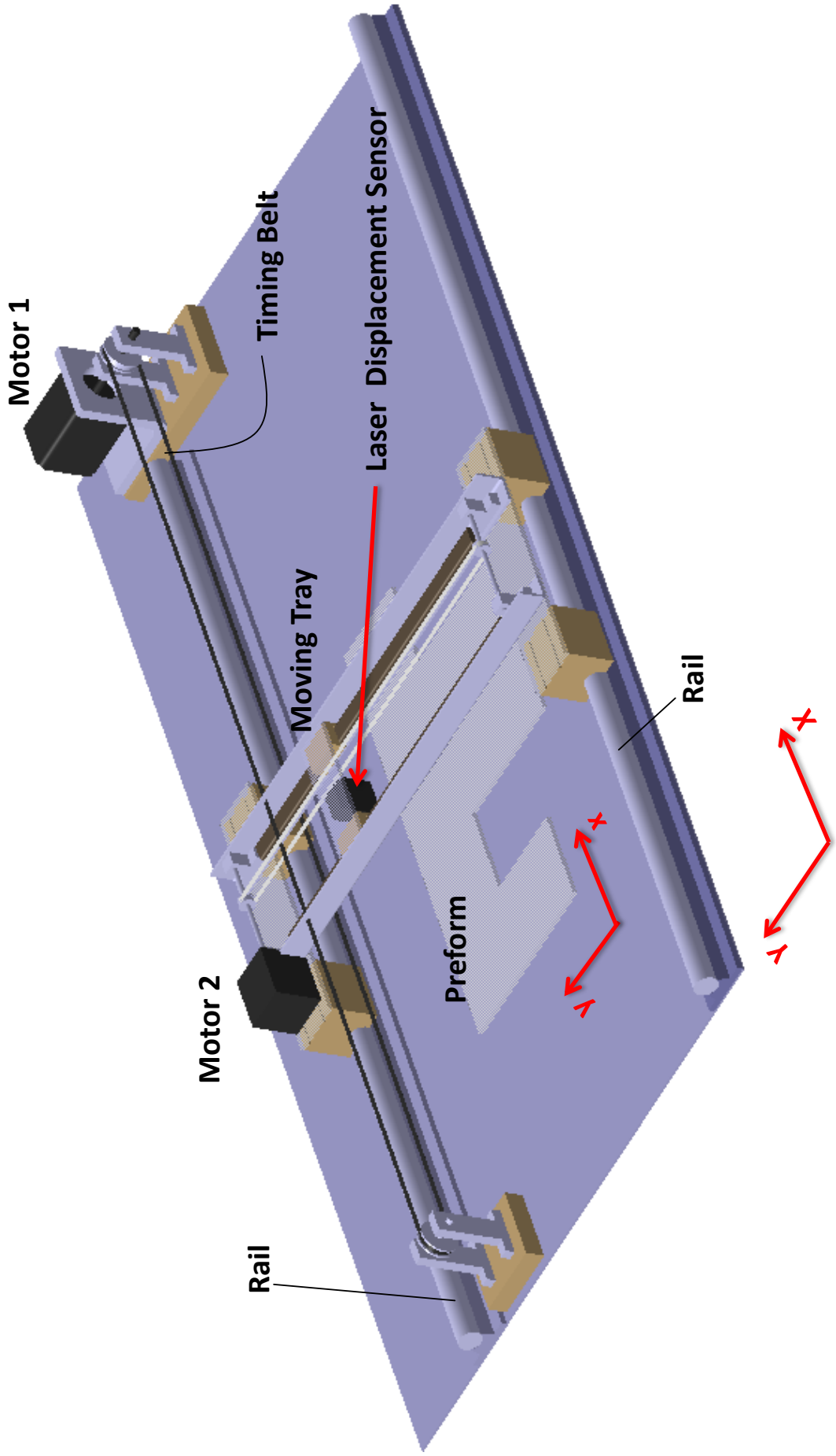

Figure 15 Experimental Setup

An Alcatel Pascal 2010 SD vacuum pump is used to apply vacuum. The vacuum pump is connected to a SMC ITV2090 regulator for pressure control. Another regulator of the same type is connected to the injection gate and it allows controling the pressure at the inlet. Vacuum pressure can be varied between 0 kPa and 80 kPa using regulators.

An NI PCI-6035E data acquisition card with 200kS/s, 16-bit, and 16 analog inputs is used for the thickness measurement of the laser displacement sensor. A Matlab GUI is used as the computer interface.

4.3.2 Material: Fabrics, Distribution Medium and Resin

In all experiments, 8 layers of random Fibroteks F50 e-glass fabrics with 450 $\mathrm{g/m^2}$ superficial density per layer are used., Polypropylene core Metyx Meticore 180 PP with 150 $\mathrm{g/m^2}$ superficial density is used as the embedded distribution media. The distribution media is placed in between glass fiber layers. Four layers of fabric are situated below the distribution media and the other four layers are situated above. Instead of actual resin, corn syrup is used. The syrup's viscosity is adjusted to 190 mPa-s by diluting it with water.

4.4. Experiments

Experiments with control actions have been conducted by Yenilmez et al. [1] for VI applications with one dimensional flow. In their paper, the thickness variation for a conventional VI with bleeding, experimentally found to be 5.44 %. After the control actions (by adjusting the

boundary conditions at the two ends, and also introducing an inner gate as explained in [1]) the thickness variation was decreased to 0.34 %. In this paper, control actions were implemented for 2D experiments. To create a 2D flow, a complex shape, vaguely similar to letter F was chosen. The outer in-plane dimensions of the fabric preform were 500 x 250 mm, and it was located on the mold as shown in Figure 18. Irregularity of the part shape combined with line injection from a single edge resulted in a 2D flow. Part's dimensions and locations of ventilation and injection ports are shown in figure 19. Two ventilation ports were selected considering a complete mold filling (i.e.,no macroscale void remaining in the mold when the resin reaches the ports). The experiment without any control action will be called Case A; and the experiment with control actions will be called Case B and Case C. Results of these three cases will be used in the next section for comparison.

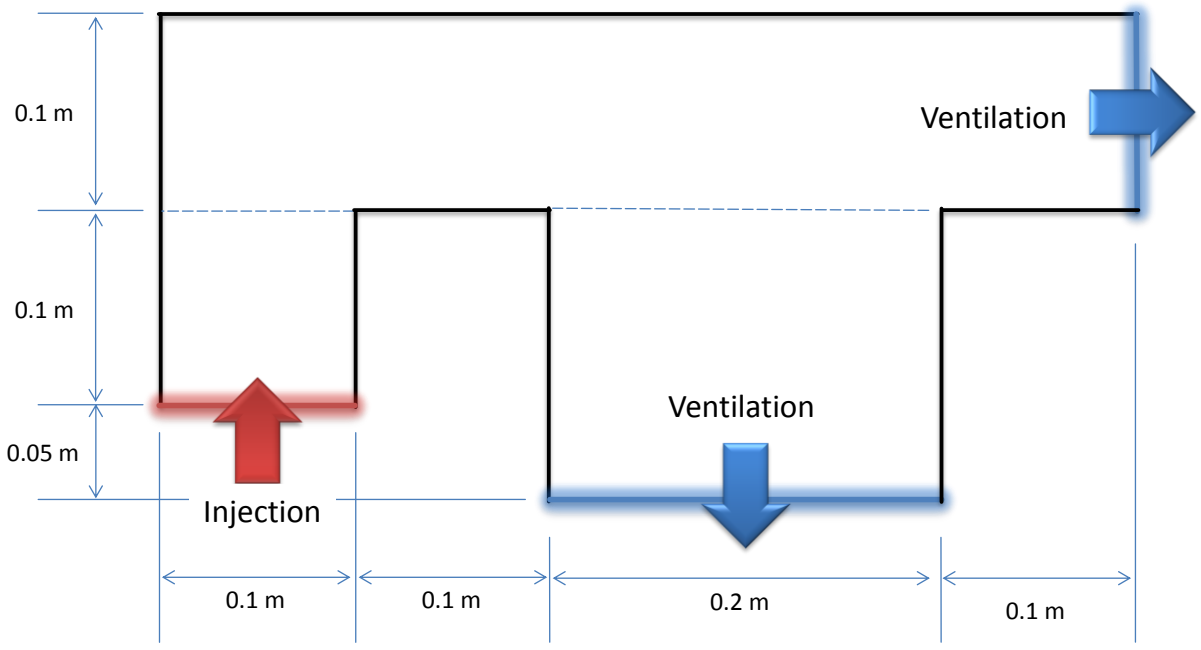

Figure 16 Preform dimensions and locations of injection and ventilation ports for Case A in which no control action will be taken. Multi-purpose Gate D, shown in Figure 2, is not active for Case A and hence is not presented here.

4.4.1 Case A: 2D Experiments Without Control Actions

In Case A, an experiment without any control action was used to demonstrate the thickness variation that occurs in a conventional VI process. The thickness was expected to be maximum at the inlet and minimum at the vent because the resin pressure is maximum at the inlet and minimum at the vent. Thus, the compaction pressure is the minimum at the inlet and maximum at the vent. This causes a spatial thickness variation such that it decreases from the inlet to the vent.

To demonstrate the plain effect of control actions of Cases B and C, bleeding was used in all cases (including Case A). Since the effect of the bleeding on final thickness variation is present in all experiments, the thickness variation difference between controlled and uncontrolled experiments can be attributed to control actions alone.

Bleeding was used to bleed excess resin by closing the injection while running the vacuum pump at the vent side. After closing the injection gate, the pressure gradient inside mold cavity started to decrease and given enough time the pressure will equalize. It is known that the pressure variation is the major reason for thickness variation, however with bleeding alone eliminating thickness variation is not possible as shown in [1,12,13]. Another important factor is fabric's behavior under compression. Not only the magnitude of the compaction pressure, but also the duration of the loading would dictate its final thickness because of the viscoelastic behavior of typical fabrics used in VI. A constant thickness distribution may not be obtained after closing the injection gate and waiting for a while during the bleeding stage if different locations have different loading histories. To achieve a more uniform thickness distribution, the method proposed in this study uses a set of control actions after mold fill.

The thickness variation of Case A at $t=t_{bleeding,0}+300$, where $t_{bleeding,0}$ is the instant of the start of bleeding, is shown in Figure 6. Change in thickness, ΔH is formulized as ΔH = H(x,y,t) – H(x,y,0) where H(x,y,t) is the instantaneous thickness and H(x,y,0) is the initial thickness distribution. As mentioned previously, the setup has the capability of scanning the mold in 29 seconds. As a result, change in thickness for a point is measured with intervals of 29 seconds.

For Case A, the maximum thickness variation percentage is calculated using the following formula:

$$\Delta H_{var}(t) = \frac{[H(x,y,t) - H(x,y,0)]_{max} - [H(x,y,t) - H(x,y,0)]_{min}}{[H(x,y,t)]_{average}} \quad (12)$$

For Case A, maximum thickness variation percentage calculated at $t_{Mold\ Fill}$ + 300 seconds,is $\Delta H_{var}(t_{Mold\ Fill+300}) = ([-0{,}17] - [-1{,}53])/3.96$ = 0,3434 = 34.3%. The standard deviation for thickness in Case A is 0.98.

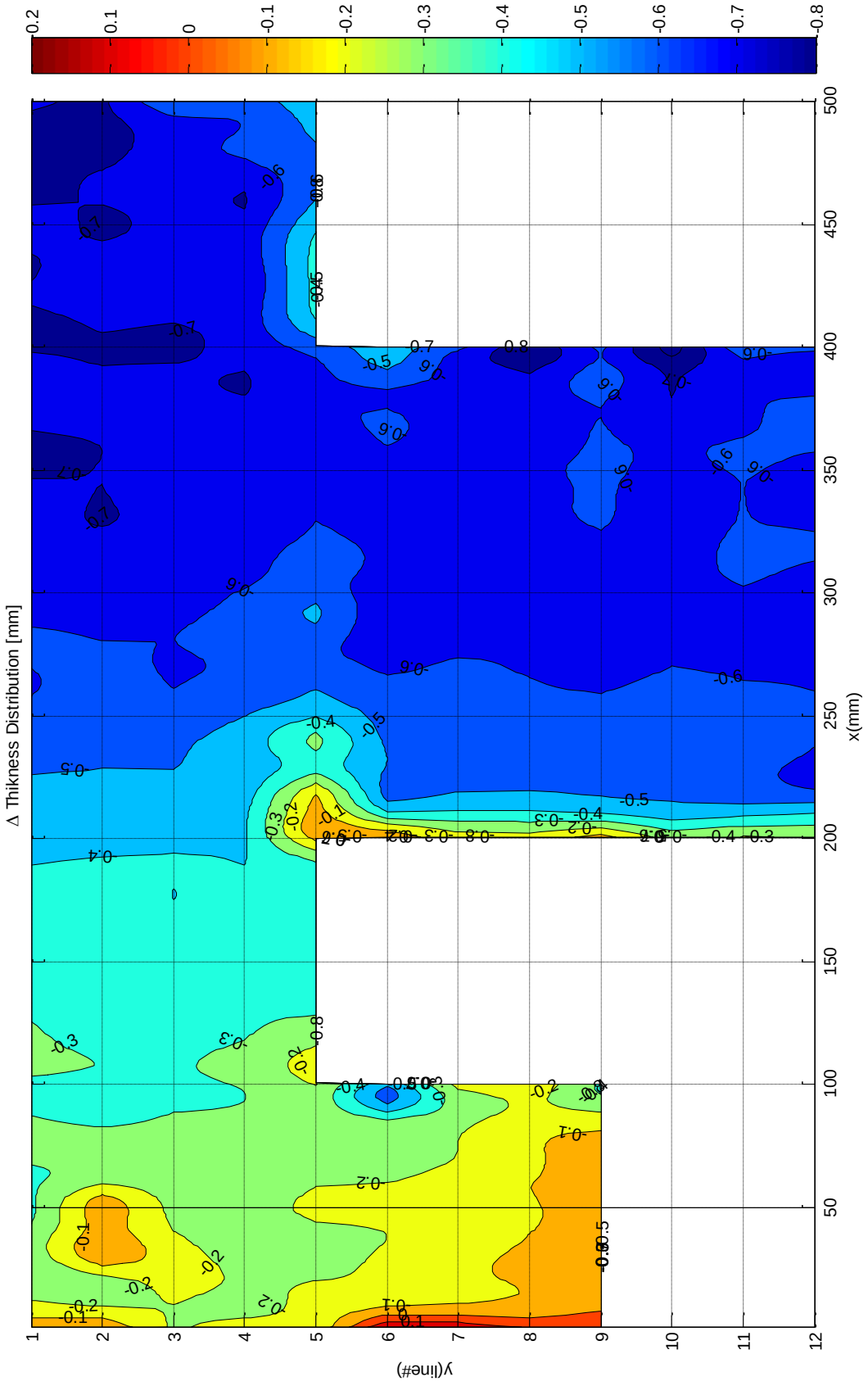

Figure 17 Change in thickness variation for t = time of mold fill

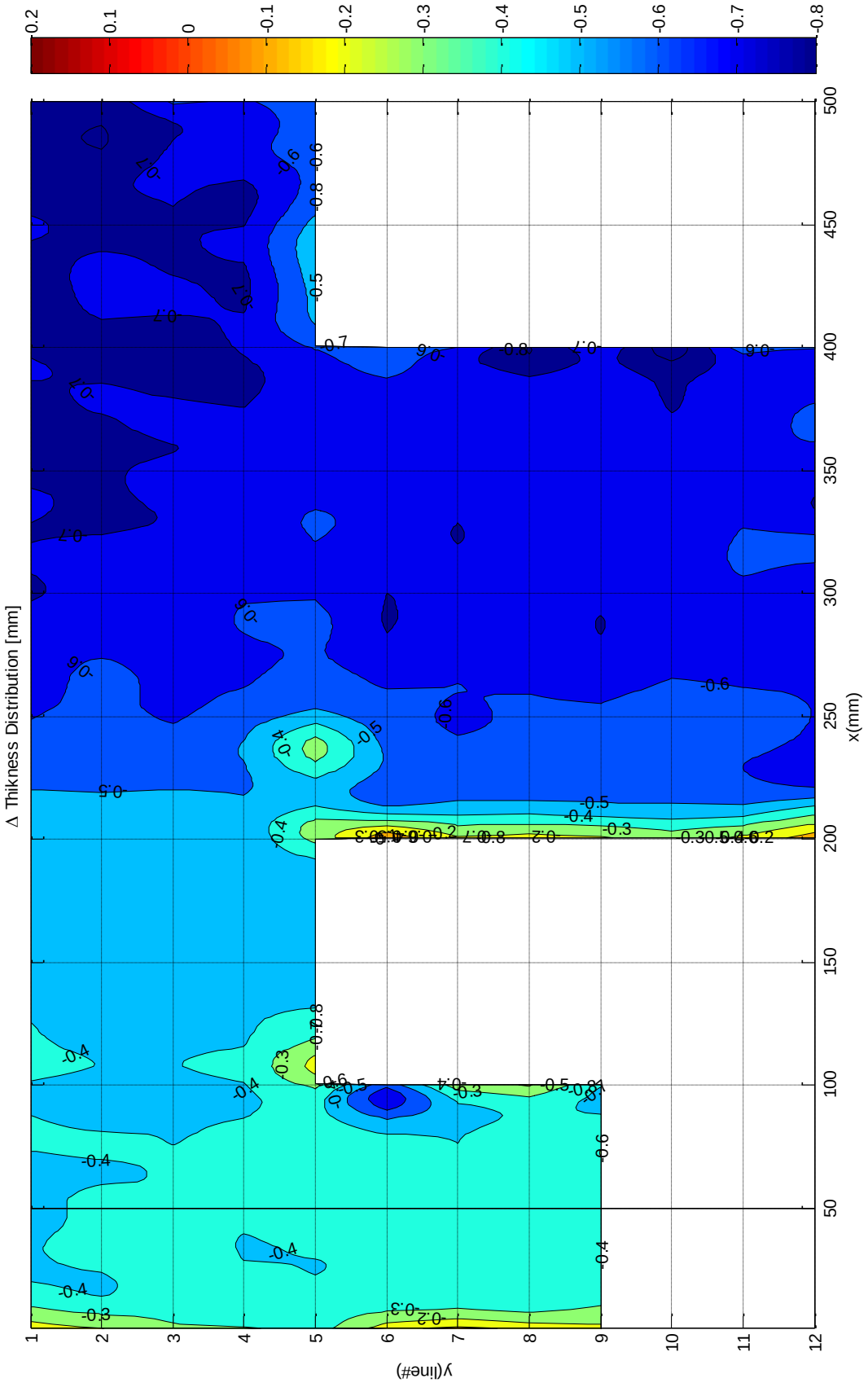

Figure 18 Change in thickness variation for t = time of mold fill + 300 seconds

4.4.2 Case B: 2D Experiments With First Set of Control Actions

In case B, in addition to bleeding, control actions were used to decrease the thickness variation. Control actions based on the FDM results of Case 4 were applied after the mold was filled completely. The same inlet and outlets were used as in Case A until the mold filling. Gate D was introduced to the system after mold filling, and it was located on the upper edge of the preform as shown in Figure 4. Before the experiment, FDM results were investigated for different scenarios and the most promising cases were selected considering the compaction/decompaction characteristics of the fabric and core types as previously studied in [2]. Same infusion parameters were used for Case B as in Case A. Control actions of Case B are tabulated in Table 2 and detailed below:

- Control Action 1: 120 seconds after the complete mold filling ($t^* = t_{CA1} / t_{MF}$= (600+180)/600 = 1.2, where t_{CA1} is the time of Control Action 1 and t_{MF} is the mold filling time), Gate D located on the upper edge of the F-shaped preform (see Figure 2), was opened and its vacuum trap pressure was set to 60 kPa. The location of Gate D was closer to the injection port (Gate A) than the other ventilation gates (Gates B and C). As a result, compaction pressure of the injection area will increase and excess resin located around the injection port will be relocated towards Gate D. The thickness is expected to decrease in the injection area and increase towards Gate D, evening previously non-homogeneous thickness distribution.
- Control Action 2: It took place 240 seconds after the mold filling ($t^* = t_{CA2} / t_{MF}$= (600+240)/600 = 1.4). In this control action, ports B and C, which were previously used for ventilation, were reverted to injection ports. Vacuum connections of ports were disconnected and they were connected to a resin reservoir which was open to atmosphere. Before reverting these ports from ventilation to injection, areas near ventilation Ports B and

C were the locations where the thickness was lowest. This is because of the high vacuum pressure in these areas. By reverting Gates B and C from ventilation to injection, resin will be introduced to the system. Additional resin will increase the thickness of locations near Gates B and C. This will decrease thickness variation between regions near Gates B and C and regions near Gate A.

- Control Action 3: It took place 390 seconds after the mold filling ($t^* = t_{CA3} / t_{MF}$= (600+390)/600 = 1.65). Excess resin around Gate A was expected to move towards Gate D as a result of Control Action 1. However, since Gate A was still open, excess resin that moved towards Gate D was replaced by resin entering the mold. By closing Gate A, thickness around Gate A was decreased even further.
- Control Action 4: It took place 540 seconds after mold filling ($t^* = t_{CA3} / t_{MF}$= (600+540)/600 = 1.9). Bleeding was applied by closing Gates B and C (Gate A was already closed in Control Action 3 and Gate D is used as ventilation). It is expected that, as a result of Control Actions used in this Case B, a more uniform compaction history will be achieved which will result in much less thickness variation in this Case B than Case A.

Experimental results of Case B are shown in Figures 9-13. Mold filling was observed at $t = t_{MF}$ =600 seconds approximately (t^* =1). Figure 9 shows the thickness variation distribution at the mold filling time. 180 seconds after the mold filling (t^*=1.3), the first control action (Control Action 1) is applied by opening Gate D at 40kPa. Figure 10 shows the thickness distribution of the mold 60 seconds after Control Action 1, to allow the effects of the control action to settle. As expected thickness decreased around Gate D and excess resin around Gate A moves towards Gate D. Control Action 2 took place near t^*=1.4. Figure 11 shows thickness variation distribution 150 seconds after Control Action 2. As expected by reverting Gates B and C from ventilation to injection thickness around

these gates increased as resin enters the mold. Figure 12 shows thickness variation distribution 150 seconds after Control Action 3. As predicted, the thickness near Gate A decreased substantially. Bleeding is applied as the fourth Control Action. Figure 13 shows the final thickness of the part scanned 840 seconds after the mold filling time (t* = 2.4). The preform is allowed to settle for 300 seconds after the bleeding. The preform's maximum percent thickness variation 300 seconds after bleeding was $\Delta H_{var}(t_{Mold\ Fill+300}) = ([-0{,}056] - [-0{,}377])/4{,}39 = 0{,}073 = 7{,}3\%$. Standard deviation, σ of thickness variation was 0.23mm for this Case B as calculated by Equation (10).

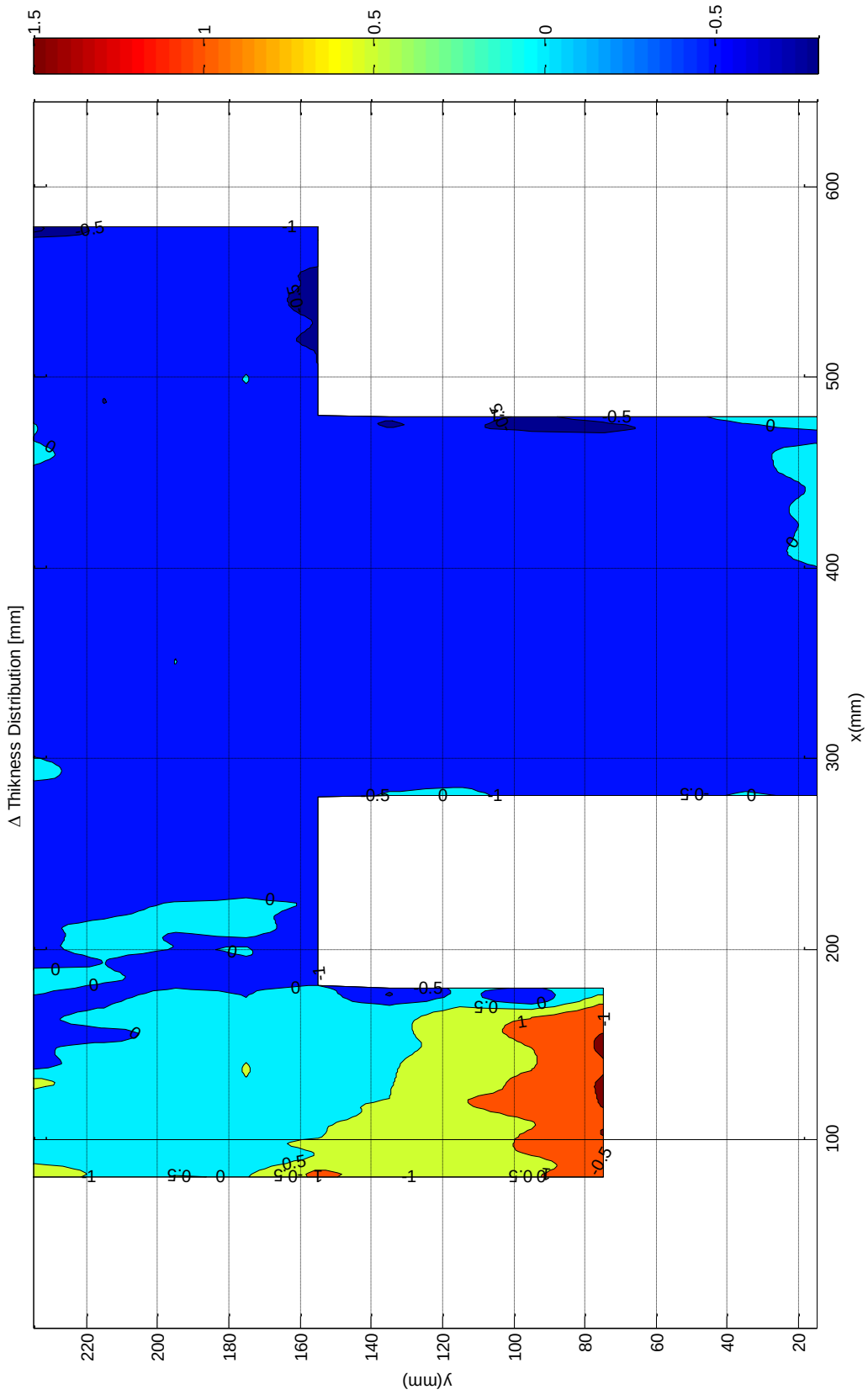

Figure 19 Change in thickness variation scanned at mold fill (t*=1)

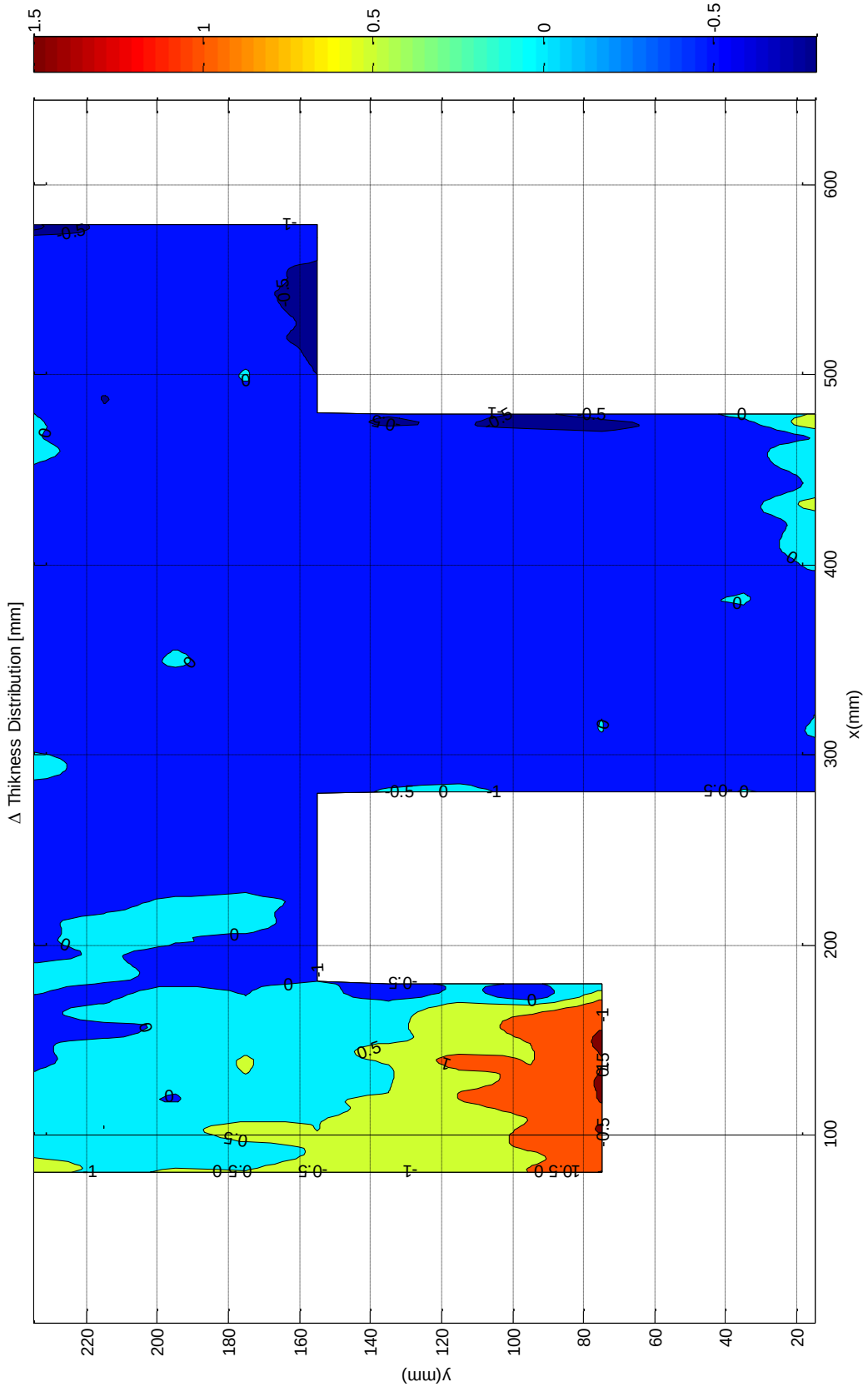

Figure 20 Change in thickness variation for Control Action 1, scanned at t = mold fill + 240 seconds (t*=1.4)

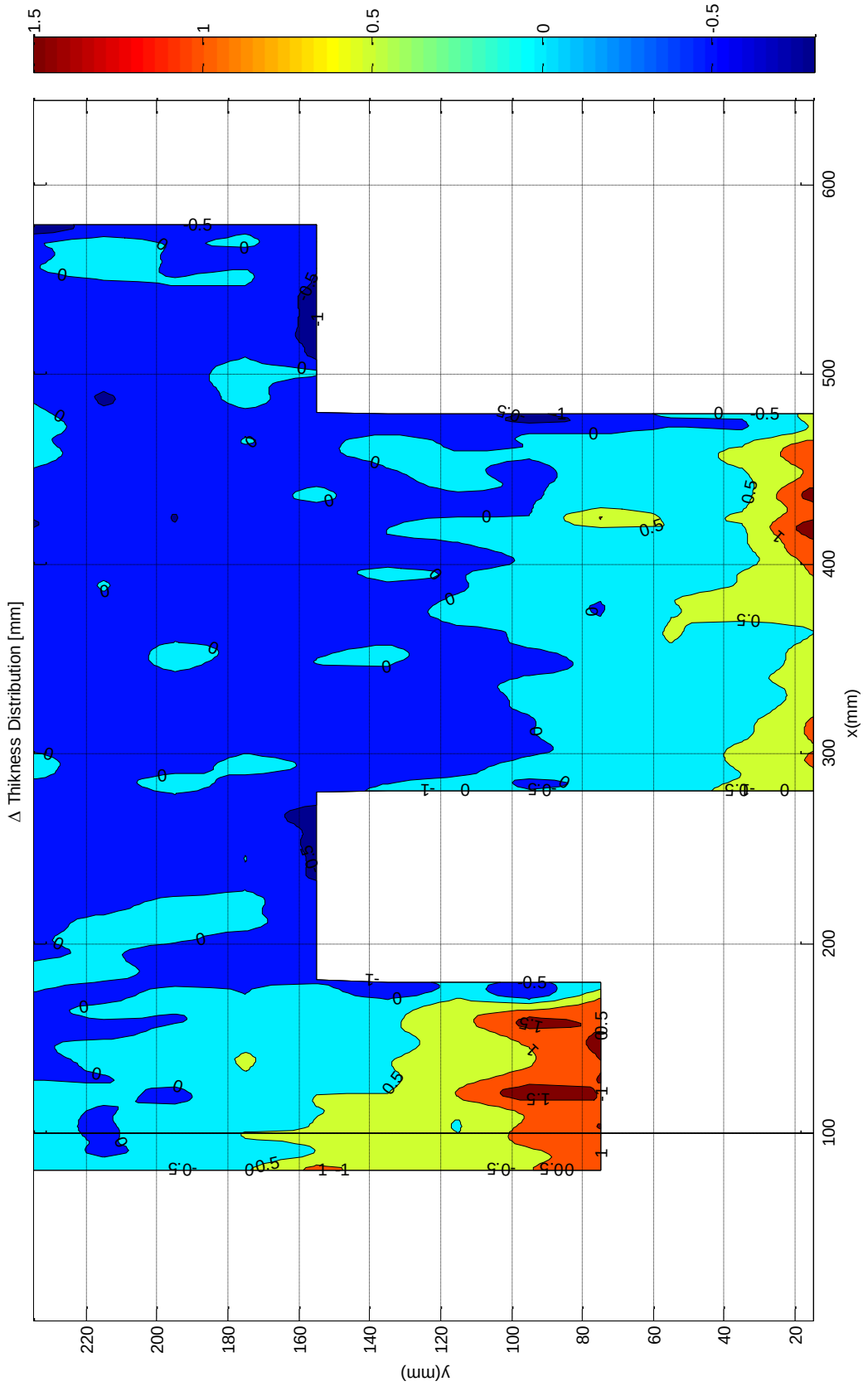

Figure 21 Change in thickness variation for Control Action 2, scanned at t = mold fill + 390 seconds (t*=1.65)

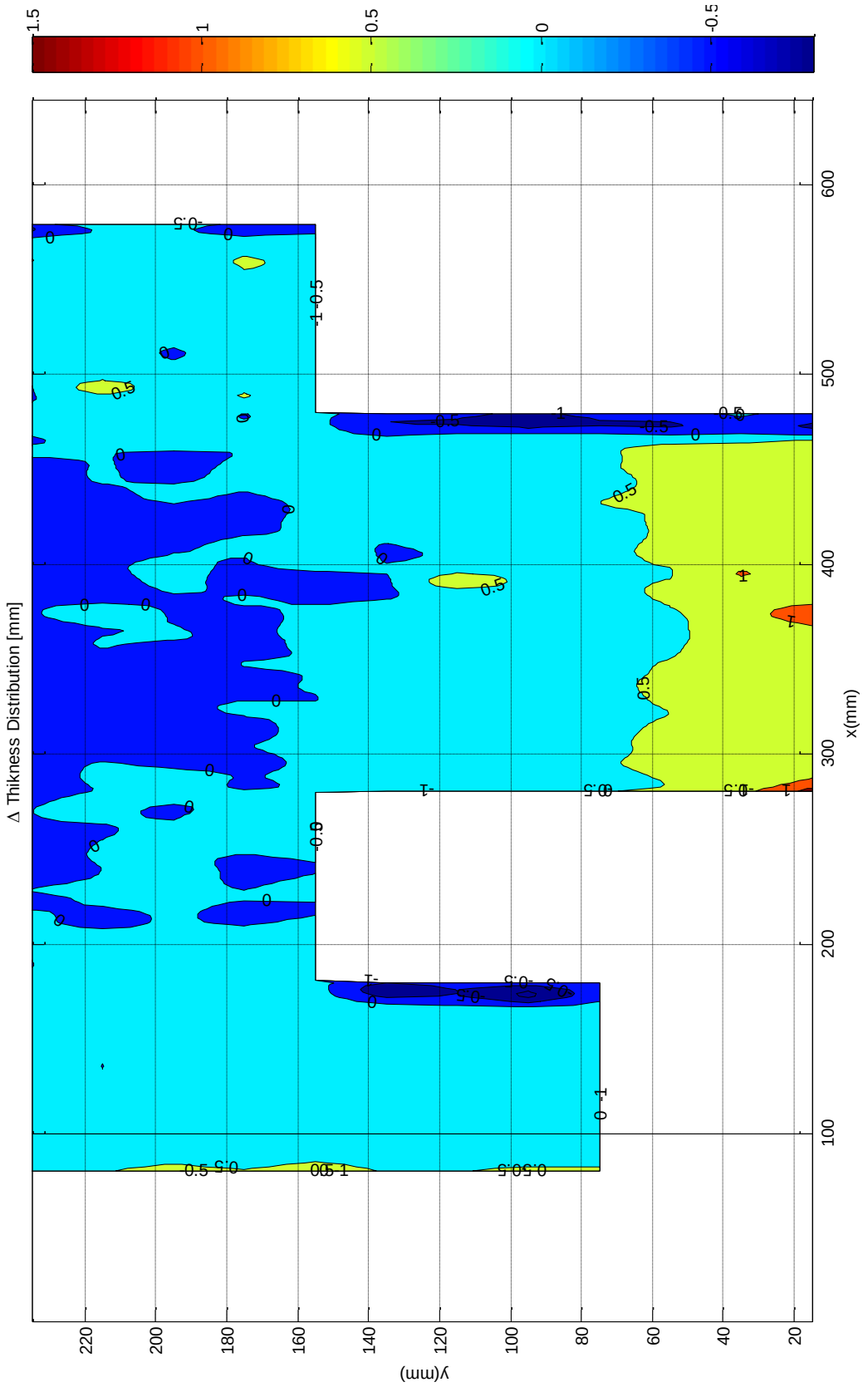

Figure 22 Change in thickness variation for Control Action 3, scanned at t = mold fill + 540 seconds (t*=1.9)

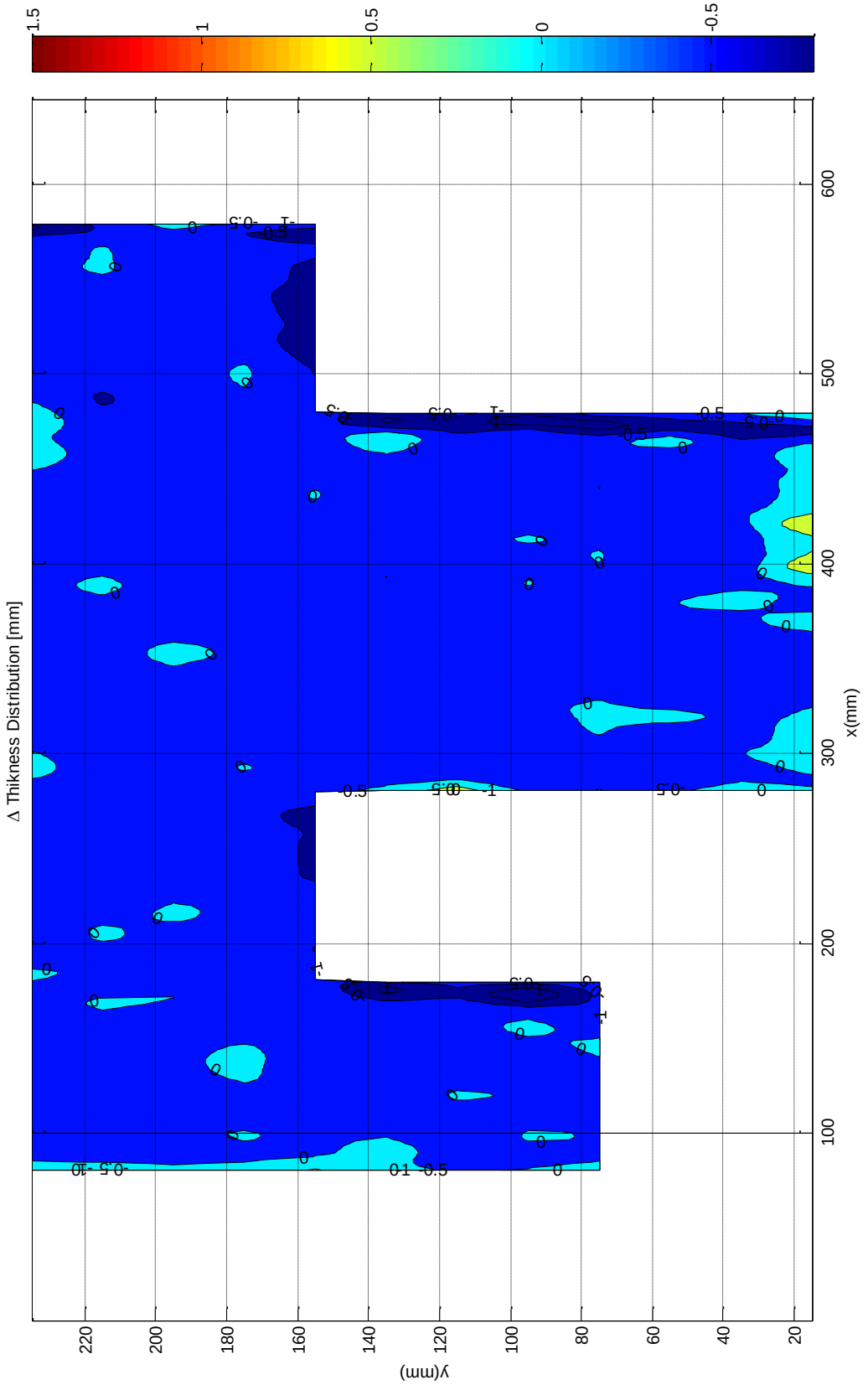

Figure 23 Change in thickness variation for Control Action 4, scanned at t = mold fill + 840 seconds (t*=2.4)

Table 3: Case B Control Actions for 2D Experiments

Action #	Non-Dimensional Time, $t^* = t/t_{MF}$	Gate A Pressure, P_A [kPa]	Gate B Pressure, P_A [kPa]	Gate C Pressure, P_A [kPa]	Gate D Pressure, P_A [kPa]	Actions	Expected Results
0	0	100	40	40	x	Injection is started from Gate A and Gate B and Gate C are used for ventilation. Gate D is kept closed.	2D resin injection
1	1.3	100	40	40	40	Gate D is activate with a pressure of 40 kPa.	Thickness on the upper part is expected to decrease
2	1.4	100	100	100	40	Gate B and Gate C pressure increased to 100kPa	Resin will start to enter to the mold from Gate B and C and increase thickness
3	1.65	x	100	100	40	Gate A is closed	Excess resin at Gate A will be relocated.
4	1.9	x	x	x	40	Gate B and Gate C are closed	Bleeding

"x" means the gate is closed.

t_{MF} denotes the time of complete mold filling, and it is approximately 600 seconds in this experiment

4.4.3 Case C: 2D Experiments With Second Set of Control Actions

Same inlet and outlets were used as in Case A until the mold filling. Gate D was introduced to the system after mold filling (Gate D was located on the upper edge of the preform as shown in Figure 4). The same infusion parameters were used Cases C and A. Similar to previous Cases A and B, bleeding was applied at the end of control actions. Control actions of Case C are tabulated in Table 3 and detailed below:

- Control Action 1: 120 seconds after the complete mold filling ($t^* = t_{CA1} / t_{MF} = (600+120)/600 = 1.2$). Gate D is activated at 40 kPa. Excess resin located around the Gate A will be relocated towards Gate D. The thickness is expected to decrease towards Gate A and increase towards Gate D, resulting in a more homogenous thickness distribution.
- Control Action 2: It took place 240 seconds after the mold filling ($t^* = t_{CA2} / t_{MF} = (600+240)/600 = 1.4$). Gates B and C were switched from ventilation to injection. Before changing these ports from ventilation to injection, areas near ventilation Ports B and C were the locations where the thickness was lowest as a result of high vacuum pressure in these areas. By reverting Gates B and C from ventilation to injection, resin will be introduced to the system. Thickness is expected to increase around Gates B and C as a result of additional resin.
- Control Action 3: It took place 390 seconds ($t^* = t_{CA3} / t_{MF} = (600+390)/600 = 1.65$). Gate D was closed. At the same time, Gate A which was used for injection previously, was converted to ventilation by changing its pressure from 100 kPa to 40 kPa. Since Gate A was used for injection during the mold filling, locations closer to the Gate A were subjected to lower compaction pressure than locations closer to ventilation gates. As a result, thickness around

Gate A is expected to be thicker than other sections. By changing it to ventilation, higher compaction pressure was applied. Excess resin, which cannot be relocated completely due to low compaction pressure, will be sucked from this new ventilation gate. Thickness around Gate A will decrease substantially, equalizing it to the thickness around Gate B and C.

- Control Action 4: It took place 540 seconds after the mold filling ($t^* = t_{CA3} / t_{MF}$ = (600+540)/600 = 1.9). Gate B and Gate C were closed for bleeding. It is expected that, as a result of Control Actions used in Case C, a more uniform compaction history will be achieved which will result in much less thickness variation in this Case C then Case A.

The mold filling time for Case C was recorded as 600 seconds (t*=1.0). Control Actions 1 and 2 were similar to Case B. Figure 11 shows the change in thickness distribution for Control Action 3 at t*= 1.9. By changing Gate A from injection to ventilation compaction pressure increased drastically. As expected, the thickness variation around Gate A decreased with increasing compaction pressure. Figure 12 shows the change in thickness distribution after bleeding. It was waited 300 seconds for the settling after bleeding. The preform percent thickness variation after 300 seconds of bleeding was $\Delta H_{var}(t_{Mold\ Fill+300}) = ([0{,}63] - [-0{,}28])/4{,}67$ = 0,1948 = 19,48% (calculated using Equation (9). Standard deviation of thickness variation, σ was 0.53mm for this Case C.

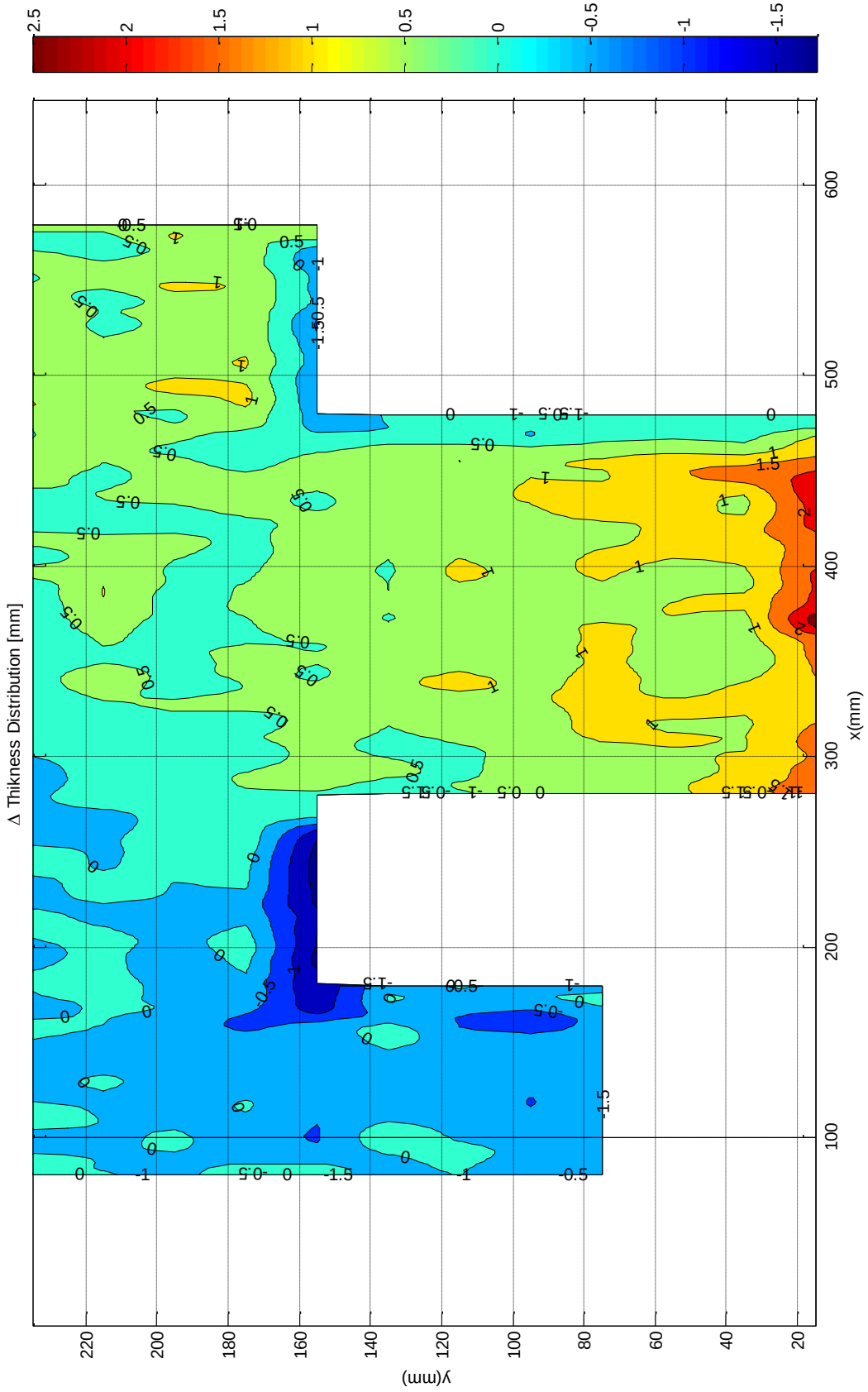

Figure 24 Change in thickness variation for Control Action 3, scanned at t = mold fill + 540 seconds (t*=1.9)

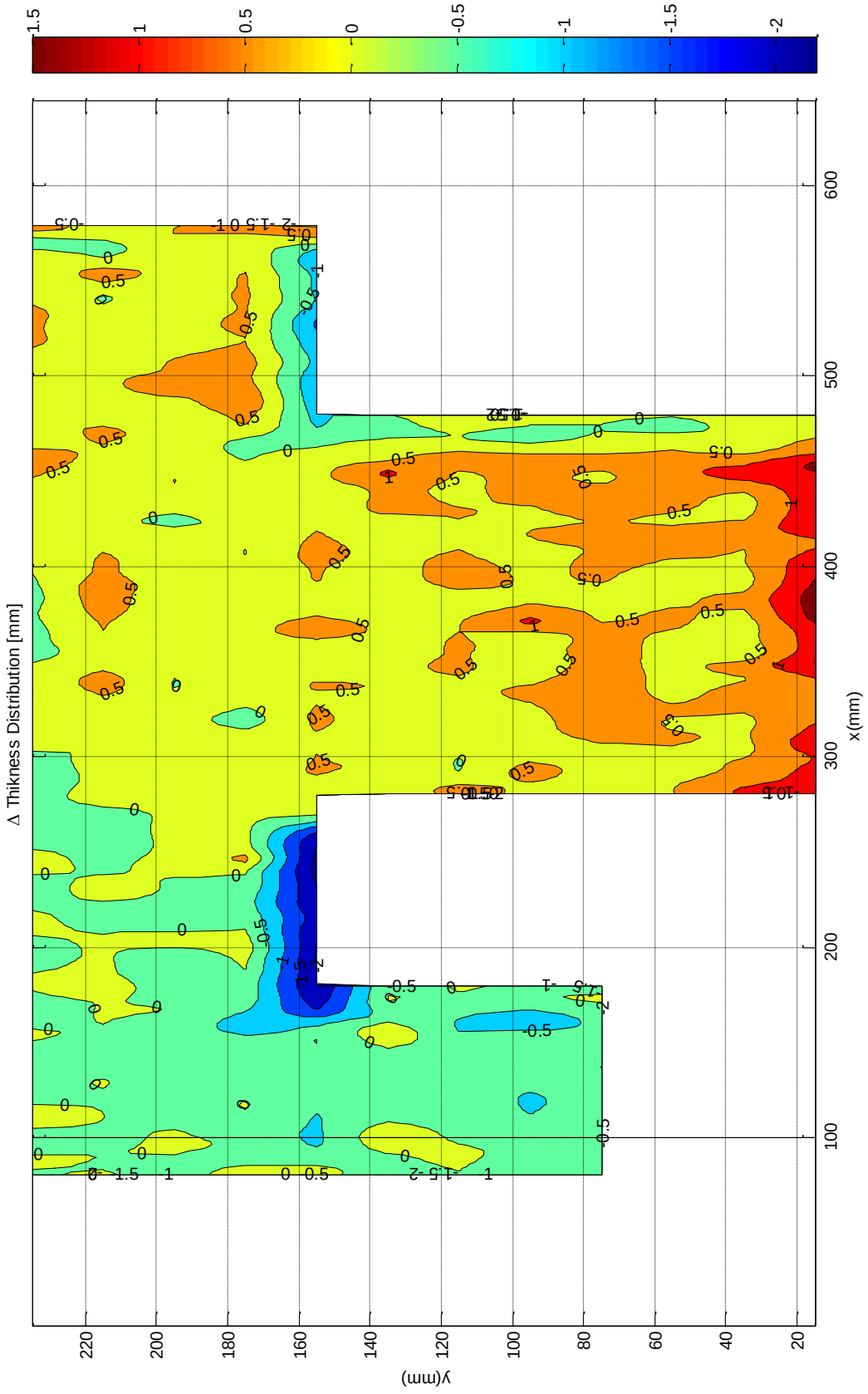

Figure 25 Change in thickness variation for Control Action 4, scanned at t = mold fill + 840 seconds (t*=2.4)

Table 4: Case C Control Actions for 2D Experiments

Action #	Non-Dimensional Time, t* = t/tMF	Gate A Pressure, PA [kPa]	Gate B Pressure, PA [kPa]	Gate C Pressure, PA [kPa]	Gate D Pressure, PA [kPa]	Actions	Expected Results
0	0	100	40	40	x	Injection is started from Gate A and Gate B and Gate C are used for ventilation. Gate D is kept closed.	2D resin injection
1	1.3	100	40	40	40	Gate D is activate with a pressure of 40 kPa.	Thickness on the upper part is expected to decrease
2	1.4	100	100	100	40	Gate B and Gate C pressure increased to 100kPa	Resin will start to enter to the mold from Gate B and C and increase thickness
3	1.65	40	100	100	x	Gate D is closed. Gate A is changed from injection to ventilation.	Thickness around Gate A will decrease due the increased compaction pressure.
4	1.9	40	x	x	x	Gate B and Gate C are closed	Bleeding

"x" means the gate is closed.

t_{MF} denotes the time of complete mold filling, and it is approximately 540 seconds in this experiment

CHAPTER 5

DISCUSSION AND CONCLUSION

The control actions considered in this study influenced the pressure distribution by introducing an additional injection gate and changing the inlet and exit pressures. The experiments shown here concluded that, introducing a gate to the system had the following effects: (i) Adding a new injection gate (i.e., an active gate with resin inflow due to a higher resin pressure value compared to the already existing gates) results in an increase in the rate of thickness change with time. (ii) Adding a new ventilation gate (a port with lower resin pressure value than already existing gates) decreases the overall thickness and rate of thickness variation with time. After the initial decrease in thickness, further compaction takes place at a slower pace. (iii) By switching a port from ventilation (exit) to injection gate (inlet) by adjusting its pressure, it is observed that the fabric relaxes slowly after a sudden drop in the compaction pressure, and it takes a long time to settle. On the other hand, it reacts much faster to an increase in the compaction pressure, caused by switching a gate from injection to ventilation, and settles down much quicker.

The previous studies showed that the thickness response of a compacted/uncompacted glass fabric is time-dependent [1,2,5]. The duration of the loading affects the thickness. For example, consider two sections in the same preform: (i) loaded under 100 kPa of compaction pressure for 15 minutes, and (ii) loaded under 50 kPa for 10 minutes and then under 100 kPa of compaction pressure for 5 minutes. Even though these initially identical sections have the same values, the corresponding thicknesses are expected to vary significantly. This explains why perfectly uniform part cannot be obtained just by bleeding the resin off; and that is why we illustrated the advantage of taking planned control actions to reduce the thickness variation.

When investigating the effect of control actions(such as changing the gate/vent pressures or closing them as in Case B) during post-filling stage, the experimental results indicate that the resin pressure and part thickness change gradually rather than settling instantaneously. The resin pressure P (and thus compaction pressure, P_c) changes with time as the fluid particles diffuse with time in the mold, instead of an instantaneous equalization of the pressure and thickness distributions just after the control action. The magnitude of the time dependency is minimized in the debulked fiber preforms (loaded/unloaded in multiple cycles). Thus, debulking prior to resin injection not only increases the fiber volume fraction, but it also helps reducing the overall variation in part thickness.

In the first part of this study (for 1D flow experiments), the thickness variation in a composite part manufactured in the VI process was inspected. An experimental setup was prepared with embedded pressure and thickness sensors to monitor the resin pressure and part thickness along a 1D flow. Two cases were presented and compared. In the first case (=

Case A), a typical infusion was made and the excess resin in the thicker regions was squeezed out by unconventional bleeding after the complete mold filling. In the second case (= Case B), control actions were proposed to reduce the thickness variation. The control actions included opening/closing injection/ventilation gates and changing the pressure of the gates. Based on the database constructed in our previous study [2], a set of control actions was planned before the experiment. As these control actions were executed, it was seen that the thickness variation was reduced compared to the uncontrolled case. For Cases A and B, the maximum thickness variations were found as 5.44 % and 0.34 %, respectively, 30 minutes after the resin gelation.

In the second part of this study (2D flow experiments), thickness variation in a complex shaped composite part manufactured by VI process was inspected. A novel experimental setup with a scanner laser thickness sensor moving in x and y axes was used to map the thickness distribution of the preform. In Case A, a typical VI experiment without control action was conducted. Bleeding was applied after the complete mold filling to squeeze out excess resin. In Cases B and C, control actions based on FDM results, were applied in the post filling stage. The control actions included opening/closing injection/ventilation gates and changing gates' pressures. By comparing uncontrolled experiments of Case A with controlled experiments of Cases B and C, it was seen that a much lower thickness variation can be obtained by applying control actions. Maximum thickness variation for Case A was found as 34.3% and standard deviation was found out as 0.98 mm. For Case B, maximum thickness variation was 7,3% and standard deviation was 0.23 mm. For Case C, maximum thickness variation was 19,5% and standard deviation was 0.53 mm. These

results suggest that, using a compaction/decompaction database and a set of control actions can be used to reduce the thickness variation.

BIBLIOGRAPHY

[1] Yenilmez, B., Senan, M., and Sozer, E.M., "Variation of Part Thickness and Compaction Pressure in Vacuum Infusion Process", *Composites Science and Technology*, 69 (2009), 1710-1719.

[2] Yenilmez, B., and Sozer, E.M., "Compaction of e-glass fabric preforms in the Vacuum Infusion Process, A: Characterization experiments". *Compos. Part A: Appl. Sci. Manuf*. 40 (2009), 499-510.

[3] Li, J., Zhang, C., Liang, R., Wang, B., and Walsh, S., "Modeling and analysis of thickness gradient and variations in Vacuum-Assisted Resin Transfer Molding process", *Polymer Composites* (2008), 473-482.

[4] Woods, J., Modin, A.E., Hawkins, R.D. and Hanks, D.J. Controlled Atmospheric Pressure Infusion Process, International Patent WO 03/101708 A1.

[5] Yenilmez, B. and Sozer, E.M., "Compaction of e-glass fabric preforms in the Vacuum Infusion process, B: Coupled model of flow and compaction", *Compos. Part A: Appl. Sci. Manuf.*, under review.

[6] Tackitt, K.D. and Walsh, SM., "Experimental study of thickness gradient formation in the VI process", *Materials and Manufacturing Processes*, 20 (2005), 607-627.

[7] Williams, C.D., Grove, S.M., and Summerscales, J., "The compression response of fibre-reinforced plastic plates during manufacture by the resin infusion under flexible tooling method", *Compos. Part A: Appl. Sci. Manuf.,* 29 (1997), 111-114.

[8] Kessels, J.F.A., Jonker, A.S., and Akkerman, R., "Fully 2,5D flow modeling of resin infusion under flexible tooling using unstructured meshes and wet and dry compaction properties", *Compos. Part A: Appl. Sci. Manuf.,* 38 (2007), 51-60.

[9] Govignon, Q., Bickerton, S., Morris, J., and Kelly, P.A., "Full field monitoring of the resin flow and laminate properties during the resin infusion process", *Compos. Part A: Appl. Sci. Manuf.,* 39 (2008), 1412-1426.

[10] Andersson, H.M., Lundstrom, T.S., Gebart, B.R., and Synnergren, P., "Application of digital speckle photography to measure thickness variations in the Vacuum Infusion process", *Polymer Composites* 24 (2003), 448-455.

[11] Modi, D., Johnson, M., Long, A., and Rudd, C., "Analysis of pressure profile and flow progression in the vacuum infusion process", *Compos. Sci. Technol.* 69 (2009), 1458-1464.

[12] Hammami, A. and Gebart, B.R., "Analysis of vacuum infusion molding process", *Polymer Composites* 21 (2000), 28-40.

[13] Andersson, H.M., Lundstrom, T.S. and Gebart, B.R., "Numerical model for vacuum infusion manufacturing of polymer composites", *Int. J. of Numer. Meth. for Heat and Fluid Flow,* 13 (2003), 383-394.

[14] Govignon, Q., Bickerton, S., and Kelly, P.A., "Simulation of the reinforcement compaction and resin flow during the complete resin infusion process", *Compos. Part A: Appl. Sci. Manuf.,* 41 (2010), 45-57.

[15] Kang, M.K., Lee. W.I., and Hahn, H.T., "Analysis of vacuum bag resin transfer molding process", *Compos. Part A: Appl. Sci. Manuf.,* 32 (2001), 1553-1560.

[16] Park, C.H. and Saouab, A., "Analytical modeling of composite molding by Resin Infusion with flexible tooling: VARI and RFI processes", *J. of Compos. Mater.* 43/18 (2009), 1877-1900.

[17] Joubaud, L., Achim, V. and Trochu, F., "Numerical simulation of resin infusion and reinforcement consolidation under flexible cover", *Polymer Composites* 26 (2005), 417-427.

[18] Acheson, J.A., Simacek, P. and Advani, S.G., "The implications of fiber compaction and saturation on fully coupled VARTM simulation", *Compos. Part A: Appl. Sci. Manuf.,* 35 (2004), 159-169.

[20] Correia, N.C., Robitaille, F., Long, A.C., Rudd, C.D., Simacek, P. and Advani, S.G., "Analysis of the vacuum infusion molding process: I. Analytical formulation", Compos. Part A: Appl. Sci. Manuf., 26 (2005), 1645-1656.

[21] Simacek, P., Heider, D., Gillespie, Jr. J.W., Advani, S.G., “Post-filling flow in vacuum assisted resin transfer molding processes: Theoretical analysis”, Compos. Part A: Appl. Sci. Manuf., 40 (2009), 913-924

[22] Yenilmez B., Akyolt T., Caglar B., Sozer E.M., “Minimizing Thickness Variation in the Vacuum infusion process: (a) use of characterization database in a model and (b) experiments”, accepted to the Journal of Composite Materials, (in print, 2012).

VITA

TALHA AKYOL was born in Ankara, Turkey on November 3, 1985. He received his B.Sc. degree in Mechanical Engineering from Koç University, Istanbul in 2009. Since then, he has enrolled in the M.Sc program in Mechanical Engineering at Koc Unıversity, Istanbul as both a teaching and research assistant. His most recent thesis, “Minimizing Thickness Variation in the Vacuum Infusion (VI) Process with 1D and 2D Resin Flows” acts as a complement to his numerous other VI related works. He is planning to continue his career as a mechanical engineer in the industry.

Appendix A.1 Experiments with flow mesh as the distribution Medium

Case C: VI Experiment using flow mesh, with No Control Action but Only Bleeding of Resin during Post-Mold Filling

In experiments using flow mesh due to low pressure deviation over the flow mesh, thickness variation over this region is also low. Covering the manufactured part completely with flow mesh is not a practical approach due to saturation problems. In such a case, the flow mesh reacts as a race tracking channel and the lower layers of perform cannot be saturated effectively. As a result of saturation problem, covering the manufactured part partially with flow mesh is a common practice. The region without the flow mesh has a lower permeability than the part with flow mesh. As a result the flow is slower in the region without flow mesh and blocks the incoming flow. Since the flow is blocked in the flow direction, in-depth flow takes place in the region with flow mesh, which results in a better saturation.

In this study, for Case C, the flow mesh is placed from 0 mm to 80 mm. A shorter length for flow mesh is adapted for the simplicity of reading thickness variation because thickness change during control actions is greater without flow mesh. Similar to a regular VARTM application, Case C differs from standard applications by its practice of bleeding. After closing the inlet, thickness reading is increased momentarily at sensor positions 1 and 2. However after a short amount of time, the thickness starts to decrease as expected. The initial increase in the thickness is due to the injection effect created by the pressure which is induced by the inlet closing action. As a result, resin is forced to the mold, increasing the thickness momentarily in the sections close to the inlet (which are sensor positions 1 and 2).

However as the pressure gradient present inside the mold cavity decrease as a result of the bleeding action the thickness eventually decreases as expected.

CASE D: VI Experiment using flow mesh, with Control Actions

Similar to Case B, in Case D, control actions are applied to decrease the thickness variation within the manufactured part. Control actions are different from case B to adjust to the different characteristic of the flow mesh but infusion parameters are similar. In case D additional gate B is introduced to the system. Gate B is located between sensors 3 and 4 (at x = 170 mm). Control actions performed in Case D are pre-defined using compactions-decompaction characteristics of preform and data obtained from Case C. Control actions are tabulated in table 2.

Control Action 1: It took place 1 minute after the complete mold filling. Gate B is activated with a pressure of 100 kPa (opened to atmosphere). By opening Gate B additional resin is introduced to the system. The additional resin will be effective in the section closer to the vent, increasing the thickness in that region. Sections closer to the ventilation were thinner than section closer to the injection gate so the increase in the thickness in the projected region is decreasing the thickness variation.

Control Action 2: It took place 3 minute after the complete mold filling. Gate A's pressure was decreased to 20 kPa, and Gate B's pressure was decreased to 40 kPa. The direction of the flow between injection gate and vent is reversed meaning the flow is from the initial vent to the initial injection gate. The part is subjected to increased compaction pressure, decreasing the thickness.

Control Action 3: It took place 5 minute after the complete mold filling. It was done to bleed out the excess resin. Similar to case B, a more even compaction history is expected due to previous control actions performed.

Appendix 1.2 Table 2: Control actions taken in case D,

0	0	100	X	40	Injection is started with Gate A and the vent are open and Gate B is closed.	1D resin injection (from left to right).
1	t_{MF} + 60	100	100	40	Gate B is activated with a pressure of 80 kPa (just before Action #1, the pressure at that location was interpolated as ~80kPa)	Resin entrance to the system will increase the thickness closer to the Gate C.
2	t_{MF} + 240	20	100	40	Gate A's pressure was decreased to 20 kPa	Gate A and Gate C become ventilations and Gate B is the sole inlet.
3	t_{MF} + 360	X	X	40	Gate A and B are closed.	The excess resin is forced to bleed out.

"X" means the gate is closed.

t_{MF} denotes the time of complete mold filling, and it is 1430 seconds in this experiment.

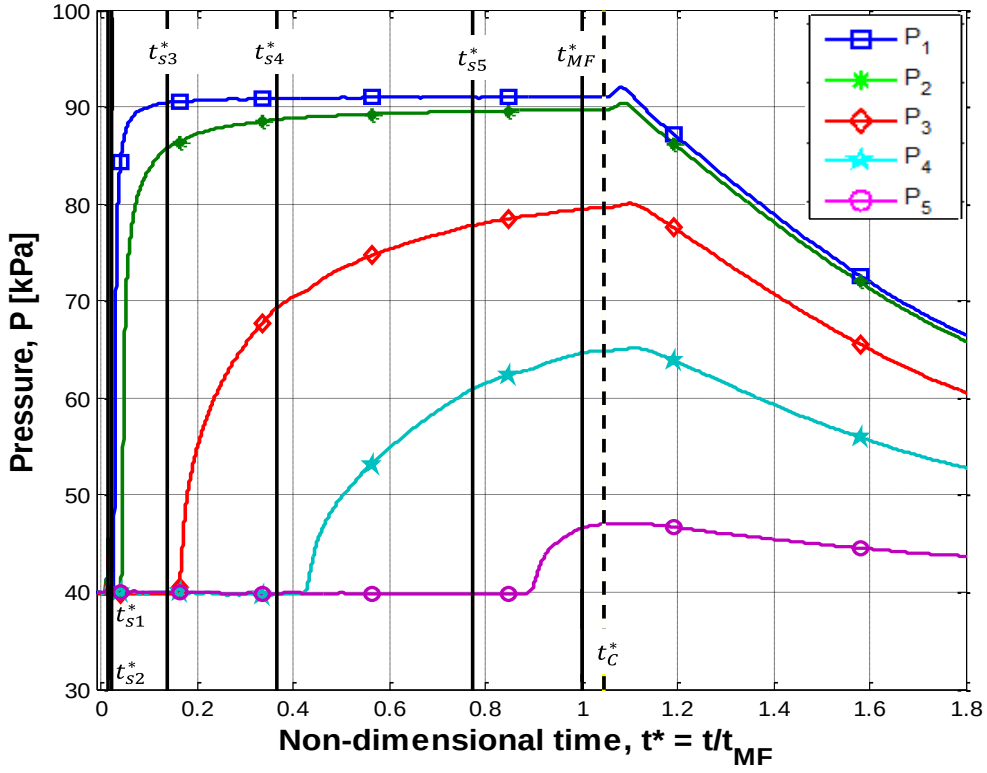

(a)

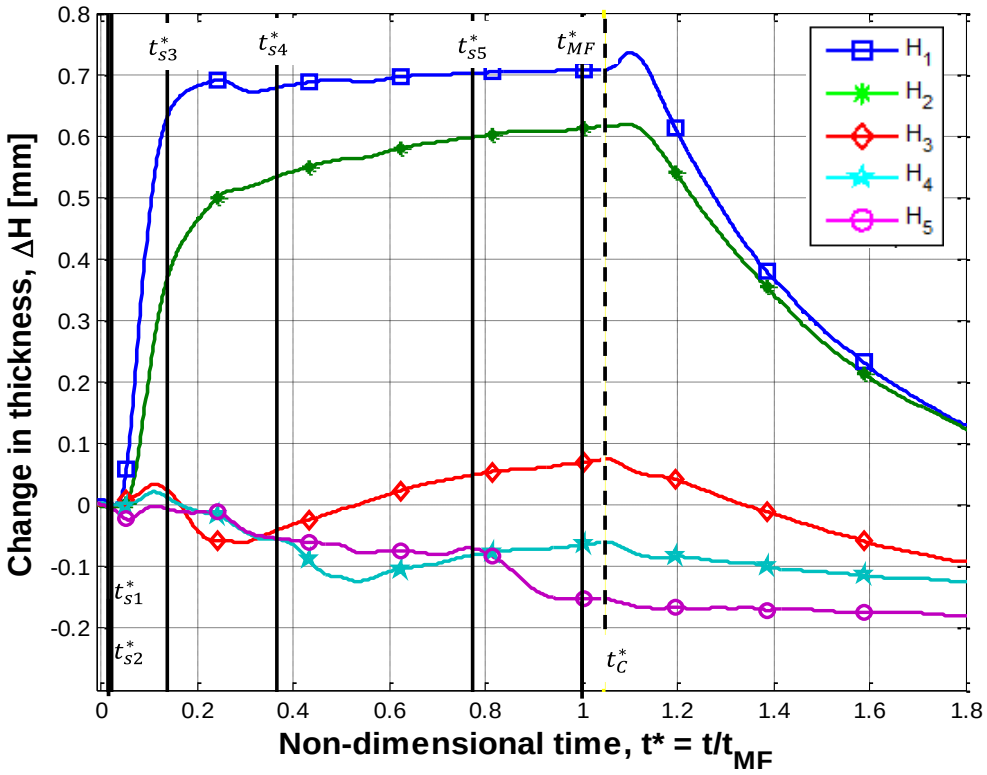

(b)

Figure 13 (a) Resin Pressure and (b): change in thickness, () for Case C. t_{si} is the resin arrival time to sensor i, and t_C is the time of the control action.

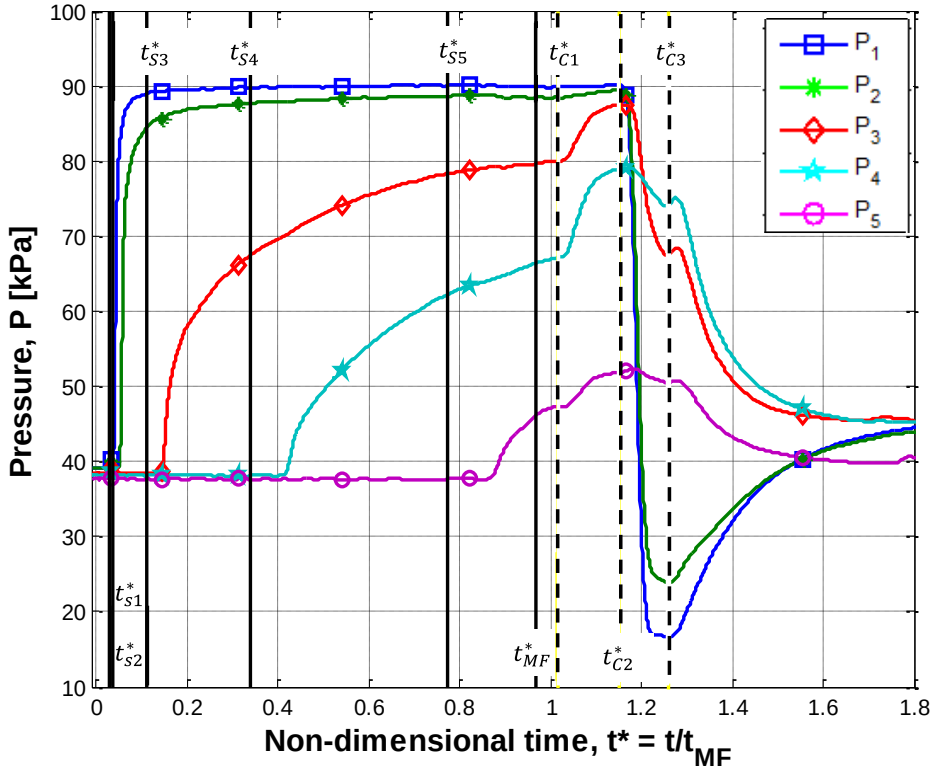

(a)

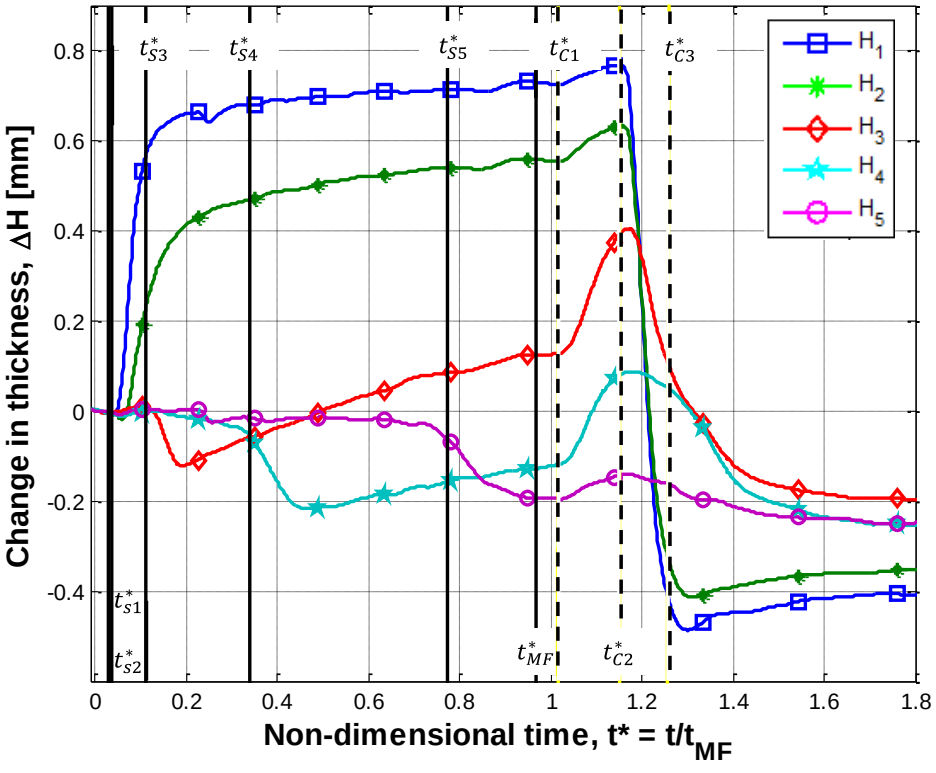

(b)

Figure 14 (a): Resin Pressure and (b):change in thickness, () for Case B. t_{Si} is the resin arrival time to sensor i, and t_{Cj} is the time of the control action j.

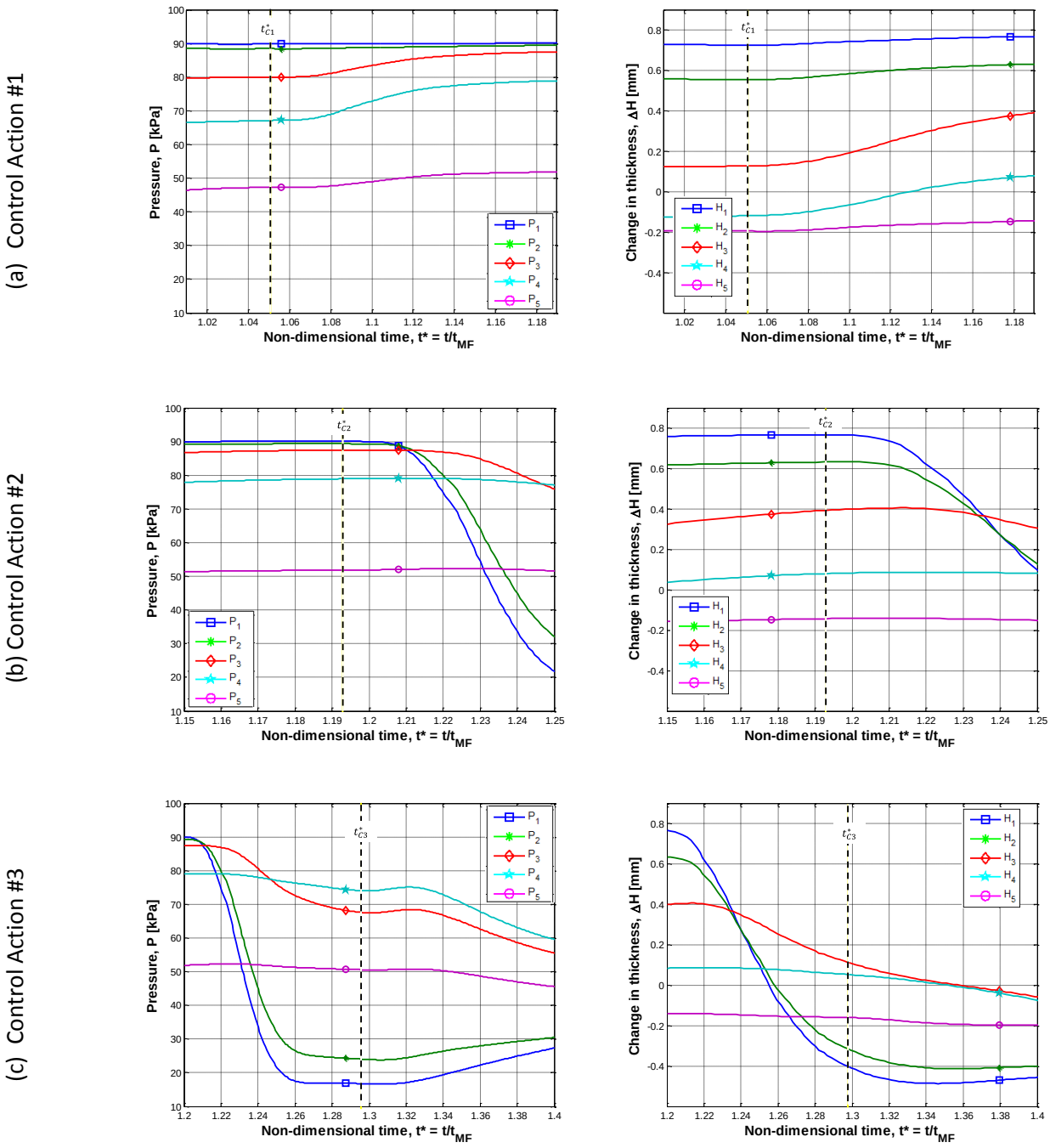

Figure 15 Pressure and thickness variations zoomed at three control actions: (a)$t^* = t_{C1}/\,t_{MF} = 1.04$, (b)$t^* = t_{C1}/\,t_{MF} = 1.23$, (c)$t^* = t_{C1}/\,t_{MF} = 1.33$. To emphasize the effect of control actions, the same P and ΔH ranges were used in all subplots. t_{Cj} is the time of the control action j.

Appendix B.1 Experimental setup for flow mesh experiments

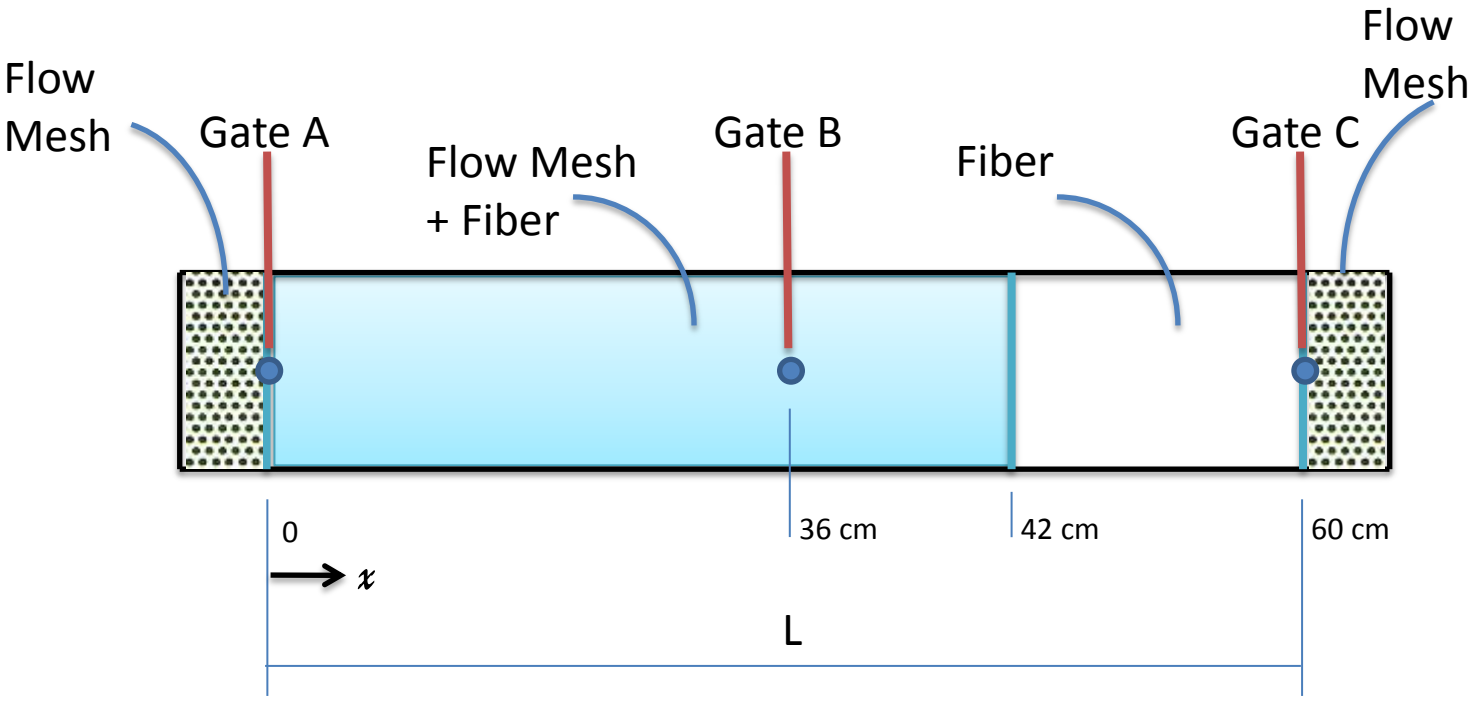

With this configuration the system has two different permeability regions. The region where flow mesh and fiber is used together (between 0 and 42 cm) has a smaller permeability value than the region consisting only fiber preform (between 48 cm and 60 cm).

Appendix B.2 Mold 3D Visualization

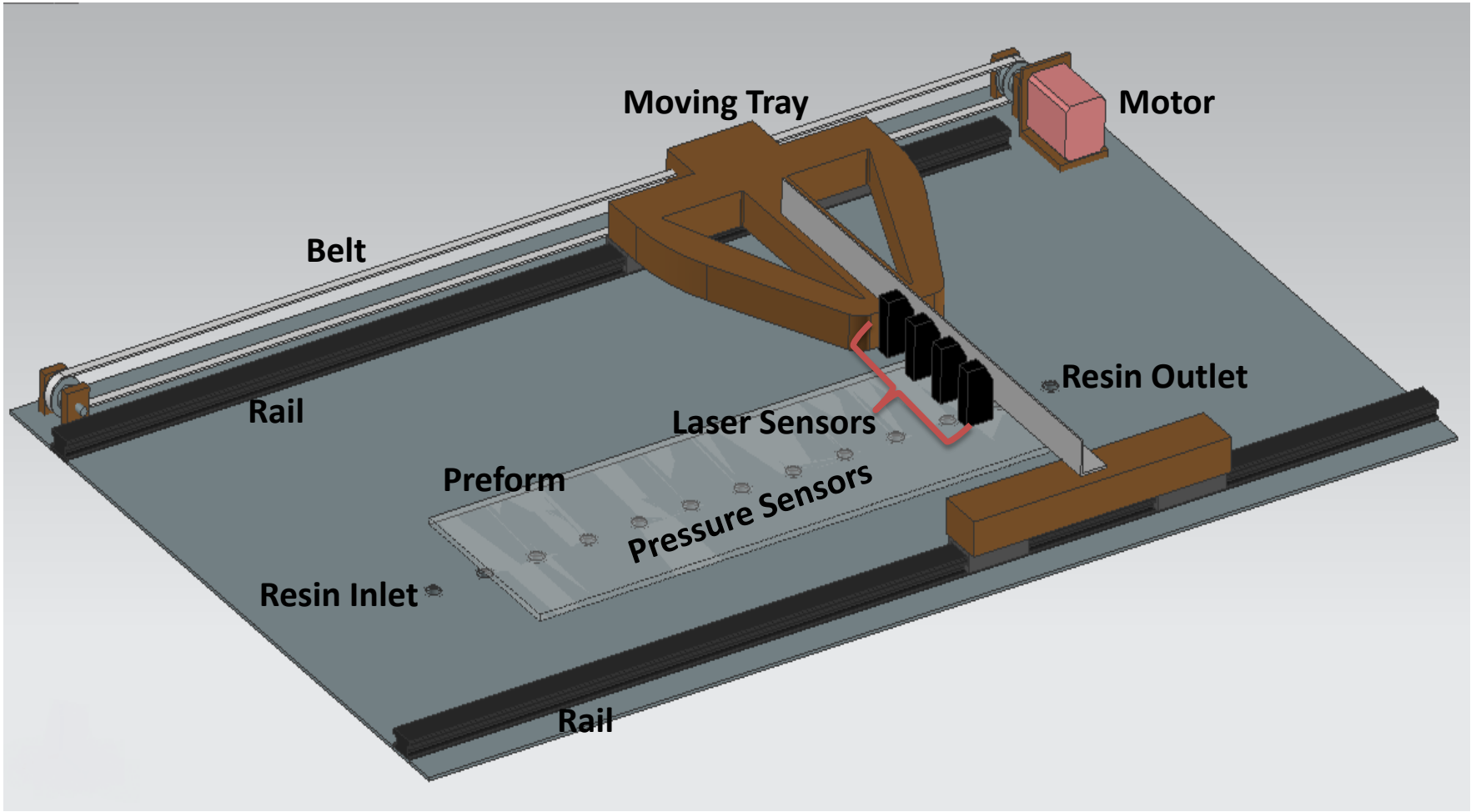

Appendix B.3 Mold Photos

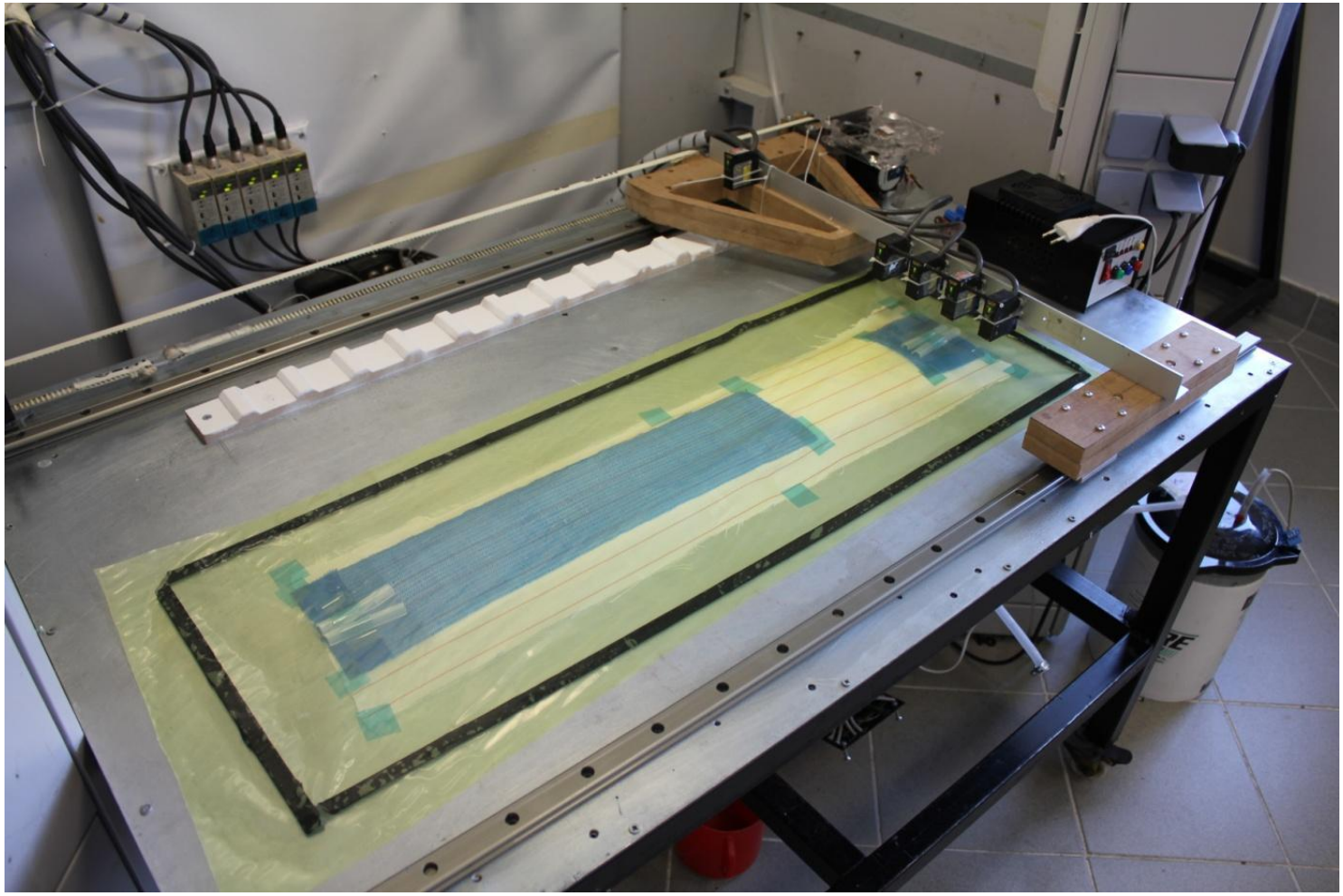

Appendix B.4 New mold 2D drawings

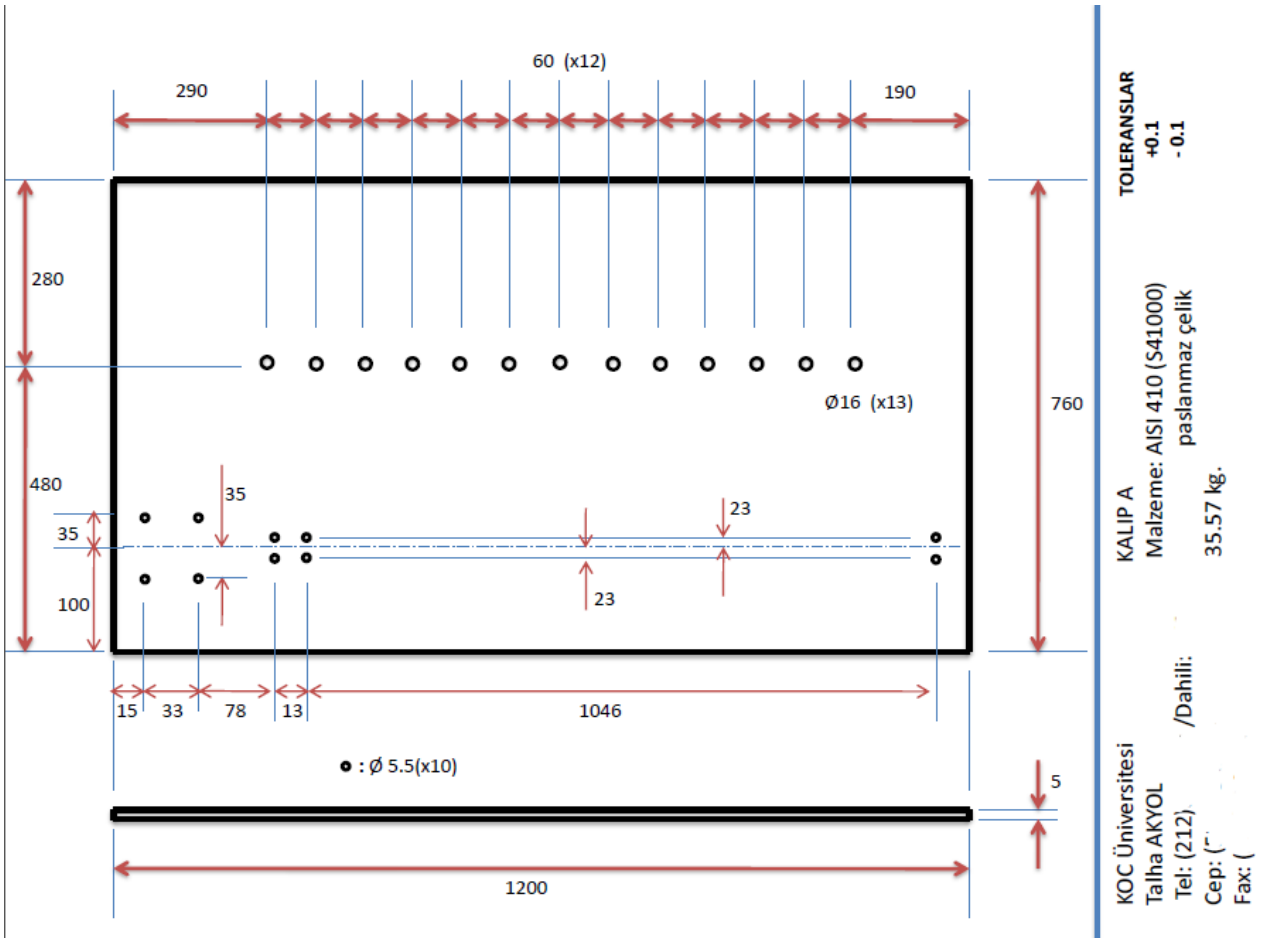

New Mold for Experiments with Flow Mesh

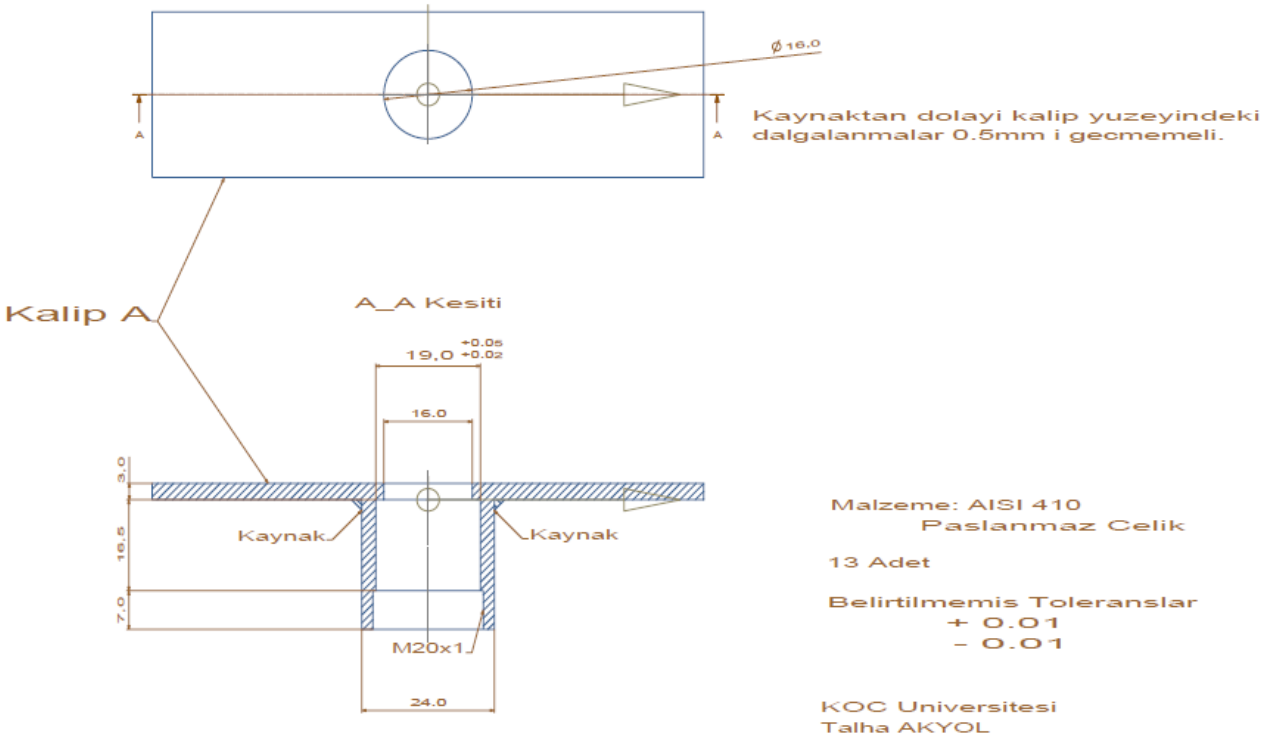

Mold and Pressure Sensor Housing Welding

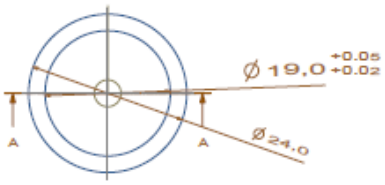

A-A Kesiti

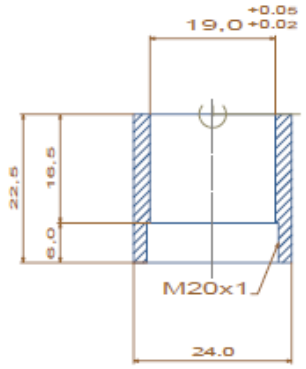

Giris Yuvasi

Malzeme: AISI 410
paslanmaz celik

13 Adet

Belirtilmemis Toleranslar
+ 0.1
- 0.1

KOC Universitesi
Talha AKYOL

Pressure Sensor Housing

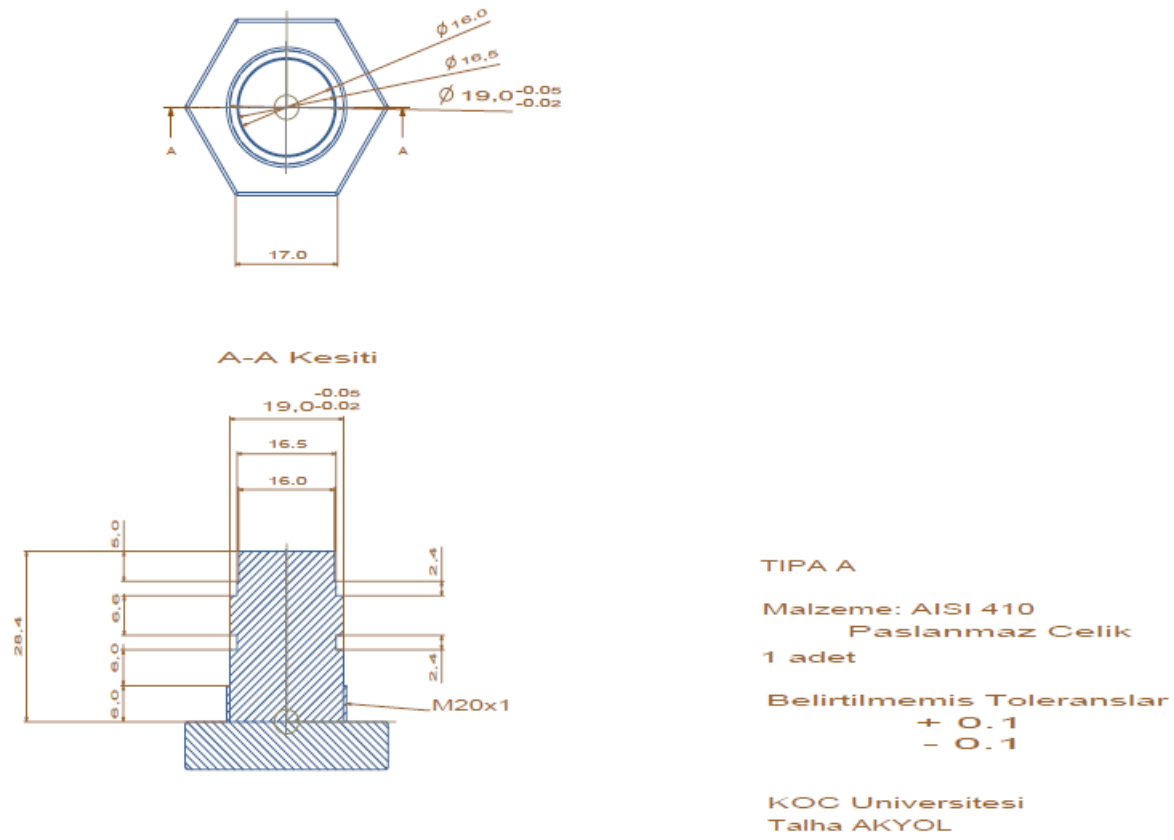

Spigot for Holes without pressure sensors

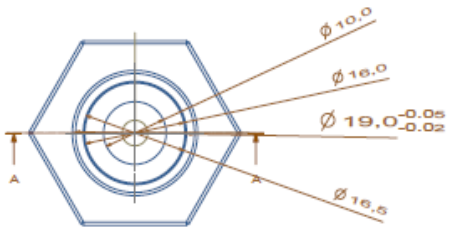

A-A Kesiti

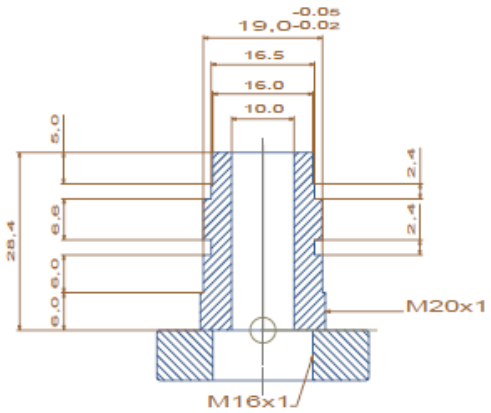

Giris Rakoru
Malzeme: AISI 410
Paslanmaz Celik
3 adet
Belirtilmemis Toleranslar
+ 0.1
- 0.1

KOC Universitesi
Talha AKYOL

Gate Spigot

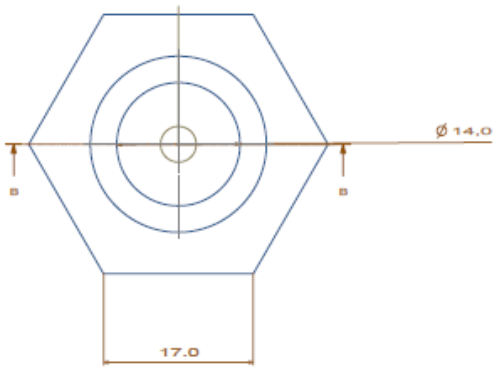

B-B Kesiti

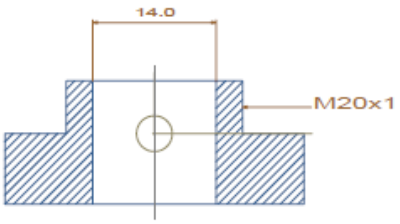

Giris Yuzugu

Malzeme: AISI 410
Paslanmaz Celik

10 adet

Belirtilmemis Toleranslar
+ 0.1
- 0.1

KOC Universitesi
Talha AKYOL

Pressure Sensor Spigot

Appendix C.1 Datasheet of the resin [www.poliya.com.tr]

Polipol™ 336-RTM

SIVI HALDEKİ ÖZELLİKLERİ
PROPERTIES OF LIQUID FORM

TEST TEST	METOD METHOD		DEĞER VALUE
Renk Colour	ISO 2211	-	max. 100 Hazen
Yoğunluk Density	ISO 1675	±%5	1,094 gr/cm³
Kırılma İndisi Refraction Index	ISO 0489	±%5	1,532
Asit Değeri Acid Value	ISO 2114	±%10	23 mg KOH/gr
Viskozite[1] Brookfield® Viscosity Brookfield®	ISO 2555	±%30	300 cp
Tiksotropi Thixotropy	-	±%30	N/A
Jel Süresi[2] Gel Time	ISO 2535	±%40	14'
Monomer Oranı Monomer Content	-	±%12	37 %
Parlama Noktası Flash Point	Abel-Pensky	-	28 °C
Raf Ömrü Shelf life in months	-	-	4 ay

1 23 °C de, 4 uç, 50 devir ile ölçülmüştür.
It is measured at 23 °C, 50 rpm with spindle 4.

2 23 °C de, % 1 ml % 1 lik Co, % 1 ml Mek-p (Butanox M 60) ile ölçülmüştür.
It is measured at 23 °C added 1 % ml Co (1 % con.) and 1 % ml Mek-p (Butanox M 60).

SERTLEŞME VERİLERİ[3]
CURING DATA

TEST TEST	METOD METHOD		DEĞER VALUE
$t_{25°C \to 90°C}$ $t_{25°C \to 90°C}$	ISO 0584	±%10	6'13"
$t_{25°C \to T\ max}$ $t_{25°C \to T\ max}$	ISO 0584	±%10	8'38"
t_{max} t_{max}	ISO 0584	±%10	11'36"
T_{max} T_{max}	ISO 0584	±%10	222 °C

3 Reçine 80 °C sıcaklığındaki banyoda, %2 oranında %50 lik Benzoil Peroksit Pasta (Lucidol BT-50,Akzo) ile sertleştirilmiştir.
Resin cured in 80 °C bath with 2% Benzoyl Peroxide Paste (50% con,Lucidol BT-50,Akzo)

SERTLEŞMİŞ REÇİNENİN ÖZELLİKLERİ [4]
PROPERTIES OF CURED RESIN

TEST TEST	METOD METHOD		DEĞER VALUE
Yük Altında Eğilme Sıcaklığı (HDT) Heat Deflection Temperature (HDT)	ISO 0075-A ISO 0075-B	±%10	77 °C 91 °C
Su Absorbsiyonu Water Absorption	ISO 0062	±%10	0,185 %
Barkol Sertliği (Barcol 934-1) Barcol Hardness (Barcol 934-1)	ASTM-D 2583	±%10	44
Toplam Hacimsel Çekme Total Volume Shrinkage	ISO 2114	±%10	9,04 %

SERTLEŞMİŞ REÇİNENİN MEKANİK ÖZELLİKLERİ [5]
MECHANICAL PROPERTIES OF CURED RESIN

TEST TEST	METOD METHOD		SAF REÇİNE DEĞERİ PURE RESIN VALUE
Eğilme Dayanımı Flexural Strength	ISO 0178	±%10	113 MPa
Elastiklik Modülü Flexural Modulus	ISO 0178	±%10	3110 MPa
Kopmadaki Uzama Elongation at Break	ISO 0178	±%10	4,3 %
Çekme Dayanımı Tensile Strenght	ISO 0527	±%10	64 MPa
Elastiklik Modülü Modulus of Elasticity in Tensile	ISO 0527	±%10	2801 MPa
Kopmadaki Uzama Elongation at Break	ISO 0527	±%10	2,8 %
Izod Darbe Dayanımı Izod Impact Strength	ISO 0180	±%10	9 kj/m^2

4 5 Sertleşmiş reçinenin testleri için reçine sertleştikten sonra post-kür işlemine tabi tutulmuştur.
Before the mechanical tests, the cured resin is post-cured.

Appendix C.2 Fabric preform material.

Fibroteks Stitched Random 500 gram/m^2

Appendix C.3 Distribution medium material.

Metyx Meticore 250PP Polypropylene core 250 gram/m^2

Appendix C.4 MPM280 Piezoresistive OEM Pressure Sensor

Features

- Pressure range 0~20kPa...35MPa;
- Gauge, absolute and sealed gauge;
- Constant current power supply;
- Isolated construction to measure various media
- Φ19mm OEM pressure element
- Full 316L stainless steel material
- Tantalum diaphragm optional;
- Different male thread connection optional

Application

- Industrial process control
- level measure
- Gas, liquid pressure measure
- Pressure meter
- Pressure calibrator
- Liquid pressure system and switch
- Refrigeration equipment and air conditioner
- Aviation and navigation inspection

Introduction

General MPM280 Piezoresistive Pressure Sensor

The outline, installation dimension and sealing method of the general MPM280 is strongly interchange, it is widely used for measuring pressure which is compatible with stainless steel and Viton;

Assembled MPM280 Piezoresistive Pressure Sensor

Put general MPM280 pressure sensor into the housing with standard or special thread; use face type seal or waterline seal; with flexible construction and serious inspecting and screening; the assembled MPM280 sensor has similar application with general type sensor, it can be used for mounting and production of different pressure instruments;

Welded MPM280 Piezoresistive Pressure Sensor

Put general MPM280 pressure sensor into the housing with standard or special thread; and weld sensor with housing together, no O-ring for sealing. The whole product has flexible construction, it has wider application fields than general pressure sensor, can be used for mounting and production of different pressure instruments;

Flush Diaphragm MPM280 Piezoresistive Pressure Sensor

Flush diaphragm pressure sensor is a full-welded pressure sensor, it has pressure port G1/2 male, sealing by Viton O-ring at the end of thread. The isolated diaphragm is welded in front of thread port, the whole measure range is 0～100kPa...35MPa. It can be used for food, medicine, sanitation fields which the media is easily dirty.

Anti-corrosive MPM280 Piezoresistive Pressure Sensor

The anti-corrosive MPM280 pressure sensor has similar outline, installation dimension and sealing methods as general MPM280 pressure sensor. For construction material, anti-corrosive pressure sensor use Tantalum diaphragm and Hastelloy C housing, and sensor type is TH (Tantalum diaphragm + Hastelloy C housing). The sensor is sealed by Viton O-ring. It can be used for strong corrosive media measurement. TH type pressure sensor's range is 0～100kPa...7MPa.

Gauge MPM280 Pressure Sensor with Vacuum Measurement

We can use general type, assembled type as well as flash diaphragm type gauge pressure sensor to measure pressure below air pressure, the min. pressure can be around -100kPa.

Electric Performance

Power supply: ≤2.0mADC
Electric connection: Kovar pin or 100mm silicon rubber flexible wires
Common mode voltage output: 50% of input (typ.)
Input impedance: 3kΩ～8kΩ
Output impedance: 3.5kΩ～6kΩ
Response (10%～90%): <1ms
Insulation resistor: 100MΩ, 100VDC
Overpressure: 1.5 times FS

Construction

Diaphragm: stainless steel 316L
Housing: stainless steel 316L
Pin: Kovar
O-ring: Viton
Net weight: ~23g（general type）
~100g（flush diaphragm）
~125g（assembled type）

Environment Condition

Position: deviate 90° from any orientation, zero change ≤0.05%FS
Shock: no change at 10gRMS, (20～2000)Hz
Impact: 100g, 11ms
Media compatibility: the gas or liquid which is compatible with construction material and Viton

Basic Condition

Media temperature: （25±1）℃

Environment temperature: （25±1）℃
Shock: 0.1g (1m/s/s) Max
Humidity: (50%±10%）RH
Local air pressure: （86～106）kPa
Power supply: （1.5±0.0015）mADC

Basic Specification

Item*	Min.	Typ.	Max.	Units
Linearity		±0.15	±0.25	%FS,BFSL
Repeatability		±0.05	±0.075	%FS
Hysteresis		±0.05	±0.075	%FS
Zero output			±2	mVDC
FS output**	70			mVDC
Zero thermal error		±0.75	±1.0	%FS, @25℃
FS thermal error		±0.75	±1.0	%FS, @25℃
Compensated temp. range		0～50		℃
Working temp. range		-40～125		℃
Storage temp. range		-40～125		℃
Stability		±0.2	±0.3	%FS/year

*testing at basic condition
**0A range, FS output ≥60mV
0B range, FS output ≥45mV
02, 03, 07, 08 absolute sensor, FS output ≥60mV
For gauge sensor which can measure vacuum, FS output ≥60mV

Outline Construction

(Units: mm)

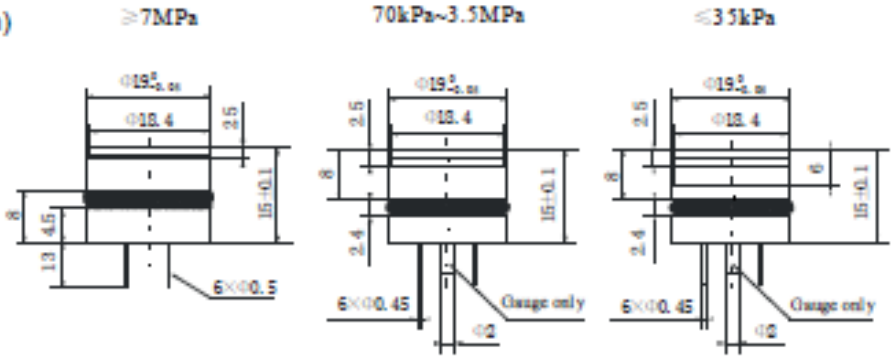

Option 0

For option 0, we suggest the installation dimension is $\Phi 19^{+0.05}_{+0.02}$ mm.

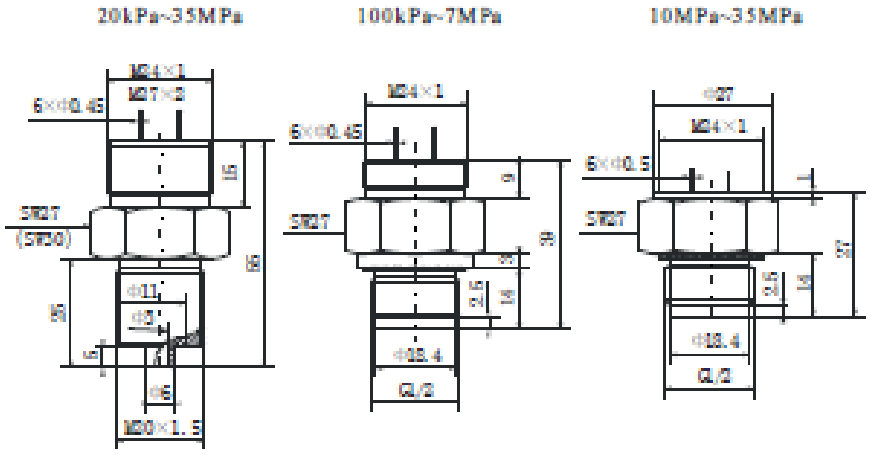

Option 1&2 Option P2

Electric Connection

Range code: 0B,0A,02,03,07,08,09,10,12,13 Range code: 14,15,17,18

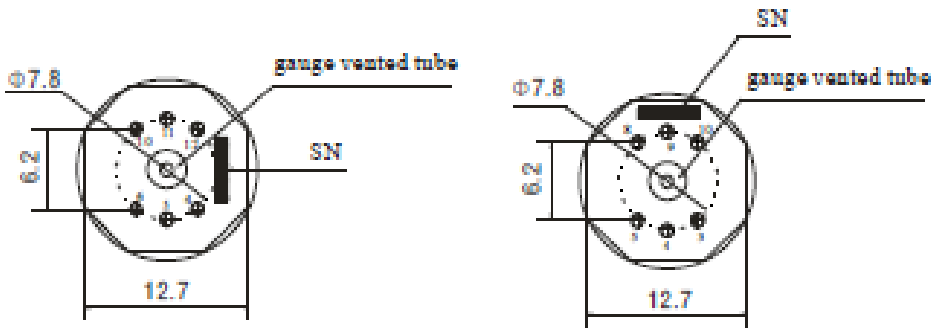

Pin	Electric connection	Wire color
4	(+OUT)	Red
5	(+IN)	Black
6	(-IN)	Yellow (while)
10	(-OUT)	Blue
Other pins are useless		

Pin	Electric connection	Wire color
4	(+OUT)	Red
5	(-IN)	yellow (white)
8	(+IN)	Black
9	(-OUT)	Blue
Other pins are useless		

Note: The actual electric connection method, please check the parameter label enclosed with products.

Order Guide

MPM280(TH)*	Piezoresistive OEM Pressure Sensor							
	Range code	Pressure range	Ref.	Range code	Pressure range	Ref.		
	0B	0~20kPa	G	10	0~1MPa	G.A		
	0A	0~35kPa	G	12	0~2MPa	G.A		
	02	0~70kPa	G.A	13	0~3.5MPa	G.S.A		
	03	0~100kPa	G.A	14	0~7MPa	S		
	07	0~200kPa	G.A	15	0~10MPa	S		
	08	0~350kPa	G.A	17	0~20MPa	S		
	09	0~700kPa	G.A	18	0~35MPa	S		
		Code	Pressure type					
		G	Gauge					
		A	Absolute					
		S	Sealed gauge					
			Code	Pressure connection	Installation			
			0 or null	O-ring				
			1	M20x1.5 male, waterline seal	Top: M24x1 male (P<2MPa)			
			2	M20x1.5 male, waterline seal	Top: M27x2 male			
			P2	G1/2 male, Waterline seal	Top: M24x1 male（female）			
				Code	Compensation			
				L	Laser trimming			
				M	Outer compensated resistor (providing resistor value)			
					Code	Electric connection		
					1	Φ0.45mm (φ0.5mm) Kovar pin		
					3	4-color flexible wire, default length:100mm		
						Code	Special measurement	
						Y	Gauge sensor to measure vacuum (0~-100kPa)	
MPM280	09	G	0	L	1	Y	The whole spec	

*: when you select Tantalum diaphragm and Hastelloy C housing, pressure sensor's type is MPM280TH;

Order Note

1. The real measured pressure should be less than 80% full scale;

2. We recommend that please do not shorten pressure range too much when the user uses the pressure sensor. That will make output signal too small to use;